E83-10253

CR-170257

SECRETARIA DE PLANEJAMENTO DA PRESIDÊNCIA DA REPÚBLICA

CONSELHO NACIONAL DE DESENVOLVIMENTO CIENTÍFICO E TECNOLÓGICO

(E83-10253) STORM-TIME CHANGES OF GEOMAGNETIC FIELD AT MAGSAT ALTITUDES (325-550 KM) AND THEIR COMPARISON WITH CHANGES AT GROUND LOCATIONS (Instituto de Pesquisas Espaciais, Sao Jose) 42 p

N83-23658

Unclas

G3/43 00253

INSTITUTO DE PESQUISAS ESPACIAIS

1. Publication Nº *INPE-2675-PRE/282*	2. Version	3. Date *Mar., 1983*	5. Distribution ☐ Internal ☒ External ☐ Restricted
4. Origin *DGA*	Program *GEOMAGNETISMO*		

6. Key words - selected by the author(s)
GEOMAGNETIC VARIATIONS
STORM-TIME CHANGES

7. U.D.C.: *550.3*

8. Title *INPE-2675-PRE/282*

STORM-TIME CHANGES OF GEOMAGNETIC FIELD AT MAGSAT ALTITUDES (325-550 Km) AND THEIR COMPARISON WITH CHANGES AT GROUND LOCATIONS

10. Nº of pages: *41*

11. Last page: *39*

12. Revised by

M. A. Abdu

9. Authorship *Rajaram Purushottam Kane*
Nalin Babulal Trivedi

Responsible author Rajaram P. Kane

13. Authorized by

Nelson de Jesus Parada
Director

14. Abstract/Notes

The values of H, X, Y, Z at MAGSAT altitudes were first expressed as residuals ΔH, ΔX, ΔY, ΔZ after subtracting the model HMD, XMD, YMD, ZMD. The storm-time variations of H showed that ΔH (Dusk) was larger (negative) than ΔH (Dawn) and occurred earlier, indicating a sort of hysteresis effect. Effects at MAGSAT altitudes were roughly the same (10% accuracy) as at ground, indicating that these effects were mostly of magnetospheric origin. The ΔY component also showed large storm-time changes. The latitudinal distribution of storm-time ΔH showed north-south asymmetries varying in nature as the storm progressed. It seems that the central plane of the storm-time magnetospheric ring current undergoes latitudinal meanderings during the course of the storm.

15. Remarks

This work is being submitted to the Journal of Geophysical Research.

STORM-TIME CHANGES OF GEOMAGNETIC FIELD AT MAGSAT ALTITUDES (325-550 Km) AND THEIR COMPARISON WITH CHANGES AT GROUND LOCATIONS

by

R.P. Kane and N.B. Trivedi

Instituto de Pesquisas Espaciais - INPE
Conselho Nacional de Desenvolvimento Científico e Tecnológico - CNPq
12200 - São José dos Campos, SP, Brasil

Abstract

The values of H, X, Y, Z at MAGSAT altitudes were first expressed as residuals ΔH, ΔX, ΔY, ΔZ after subtracting the model HMD, XMD, YMD, ZMD. The storm-time variations of ΔH showed that ΔH(Dusk) was larger (negative) than ΔH(Dawn) and occurred earlier, indicating a sort of hysteresis effect. Effects at MAGSAT altitudes were roughly the same (10% accuracy) as at ground, indicating that these effects were mostly of magnetospheric origin. The ΔY component also showed large storm-time changes. The latitudinal distribution of storm-time ΔH showed north-south asymmetries varying in nature as the storm progressed. It seems that the central plane of the storm-time magnetospheric ring current undergoes latitudinal meanderings during the course of the storm.

STORM-TIME CHANGES OF GEOMAGNETIC FIELD AT MAGSAT ALTITUDES (325-550 KM) AND THEIR COMPARISON WITH CHANGES AT GROUND LOCATIONS

by

R.P. Kane and N.B. Trivedi

Instituto de Pesquisas Espaciais - INPE
Conselho Nacional de Desenvolvimento Científico e Tecnológico - CNPq
12200 - São José dos Campos, SP, Brasil

1. Introduction

The quiet-day patterns of geomagnetic field and its periodic variations (e.g. Sq) are occasionally violently disturbed, exhibiting what are known as Geomagnetic Storms. The anatomy of such storms and their relationship with solar events have been studied for almost a century and a detailed exposition is available in the liturature, specially in the three famous books viz. by Chapman and Bartels (1940), Matsushita and Campbell (1967) and Akasofu and Chapman (1972). A typical geomagnetic storm is characterised by a sharp initial increase called Storm Sudden Commencement (SSC), which may last for a few minutes (and may be associated sometimes with a Preliminary Reverse Impulse PRI), followed by a large drop in the H component of a few hundred nT within a few hours, followed later by a slow recovery. These features have different magnitudes at different latitudes and longitudes, indicating a UT component called storm-time variation Dst, and a LT component called disturbance local-time inequality DS. From a detailed analysis of several hundred storms, Sugiura and Chapman (1960) demonstrated that whereas Dst had a pattern as mentioned above viz. SSC followed by the Main phase and the Recovery, the DS was characterised by a Dawn maximum and a Dusk minimun. Kane (1971) obtained similar results.

The source of these storm-time changes is known since long to be far away from the earth, in the form of a ring current, several earth radii away in the magnetosphere. The isotropic (symmetric) ring current causes the Dst. The asymmetric part DS was earlier thought to be due to ionospheric return currents from an extended westward electrojet in the auroral region. From spacecraft observations, Cahill (1966) and Langel and Cain (1968) concluded that the DS variations too were of magnetospheric origin. However, whether DS has some ionospheric contribution too is still a debatable question (Kane 1972, 1973, 1974). It would be of great interest if observations were available from spacecrafts above, but not very far from the ionosphere. MAGSAT provides the first such opportunity, as the spacecraft, though confined to the Dawn-Dusk sectors because of its sun-syncronization, was in the altitude range of 325-550 Km. In this communication, we report results for storm-time changes, observed by MAGSAT.

2. Data analysis

The present work pertains to the MAGSAT Project M55, entitled "Comparison of storm-time changes of geomagnetic field at ground and at MAGSAT altitudes", for which Reports Nos. 1,2,3 and the Final Report have already been submitted to NASA. Several details and Tables etc., not reproduced here, are available in those reports.

The MAGSAT Investigator B tapes supplied to us contained data for the equatorial and low latitude region only ($\pm 35^{\circ}$), and hence all the results we report pertain to low latitudes only. Values for the X, Y, Z components were available and from these the H component was computed as $H=(X^2+Y^2)^{1/2}$. Since a major part of the observed values of X(or H) was of internal origin (earth's interior) and the effects we wanted to study were of external origin and quite small (only a few hundred nT as compared to the several tens of thousands of nT of observed X or H), it was necessary to remove first some sort of a gross, background level of internal origin. The tapes contained MGST (4/81) model values XMD, YMD, ZMD which are supposed to contain no external terms. From these, we calculated $HMD = (XMD^2 + YMD^2)^{1/2}$ and further, residuals were obtained as $\Delta H = H$ (observed) - HMD, $\Delta X = X$ (observed) - XMD, $\Delta Y = Y$ (observed) - YMD and $\Delta Z = Z$(observed) -ZMD. All further analysis was conducted by using ΔH, ΔX, ΔY and ΔZ only.

The MAGSAT spacecraft was launched on October 30, 1979 into a twilight, sun-synchronous orbit, with inclination 96.76°, perigee 352 Km and apogee 561 Km. Thus, in the low latitude region, the passes were almost north-south or south-north along the Dawn or Dusk meridians. The equatorial crossings of successive Dawn and Dusk passes were about 0.8 hours apart, while successive Dawn (or Dusk) passes were about 1.6 hours apart.

A. Study of values at equatorial crossings

Values of ΔH etc. at the geographic equatorial crossing, are henceforth designated as ΔH_0 etc. Fig. 1 shows a plot of ΔH_0 (Dusk) (crosses) and ΔH_0 (Dawn) (dots) for the period Nov. 2-7, 1979 in the top frame, Nov. 8-13, 1979 in the middle, and Nov. 14-19, 1979 in the bottom frame. The conventional Dst (Sugiura and Poros, 1971) is also plotted in each frame and the Kp values are indicated by histrograms. The data for Nov. 2 do not seem to be reliable and hence are omitted from the analysis. In the interval Nov. 3-19, 1979 there was one major storm on Nov. 13-15, 1979. The following points may be noted:

a) In general, ΔH_0 is non-zero and negative. ΔH_0 (Dusk) is more negative than ΔH_0 (Dawn). However, both follow the Dst trend at least roughly and hence do seem to represent the storm-time changes.

b) During the storm-period (Nov. 11-15, 1979), ΔH_0 (Dusk) seems to show a behaviour similar to Dst; but ΔH_0 (Dawn) shows a different behaviour viz. lesser magnitude of storm-time effects, probably occurring later.

Fig. 2 shows a plot of ΔH_0 (Dusk) versus ΔH_0 (Dawn). Fig. 2(a) refers to Nov. 3-5, 1979, a moderately disturbed period. It may be noted that ΔH_0 (Dusk) and ΔH_0 (Dawn) were observed always about 0.8 hours apart and simultaneous observations were impossible. Hence, the arithmetic average of two successive values of ΔH_0 (Dawn) is plotted against the corresponding ΔH_0 (Dusk) value and vice versa. The scatter in Fig. 2(a) is rather large. The correlation coefficient for the 87 pairs of points is only $+0.42 \pm 0.09$ and the two regression lines, one with ΔH_0 (Dusk) as the independent variable (full line) and the other with ΔH_0 (Dawn) as the independent variable (dashed line), are wide apart, making different intercepts on the two axes.

Fig. 2(b) shows a similar plot for Nov. 6-10, 1979, again a moderately disturbed period. Here, some points (marked as dots) seem to fall reasonably well on a straight line, giving a good correlation ($+0.91 \pm 0.02$) for 89 pairs of points, and the upper line represents the corresponding regression line. However, there are many other points (marked as crosses) which deviate considerably from the above group. For all pairs taken together (total of 153 values), the correlation is only ($+0.71 \pm 0.04$) and the regression is represented by the lower line.

Fig. 2(c) shows a similar plot for the storm period Nov. 11-15, 1979. Here, the recovery period Nov. 14-15 is marked as crosses. Two separate regression lines are indicated, one for the main storm (Nov. 11-13) of slope <u>exceeding unity</u> and another for the recovery period (Nov. 14-15) of slope almost unity. Thus, differences in the storm-time evolution in the Dusk and Dawn sector are indicated.

Fig. 2(d) refers to Nov. 16-20, 1979, a moderately disturbed period. Here too, the scatter is large, just like in Fig. 2(a) and (b).

Thus, whereas Fig. 2(c) shows marked differences in the evolution of ΔH_0 (Dawn) and ΔH_0 (Dusk), the scatter in Fig. 2(a), (b) and (d) makes it difficult to draw any reliable conclusions. It is obvious that the ΔH_0 values are polluted by some other factors unconnected with storms.

What could be the causes for this scatter and, in general for the non-zero values of ΔH_0 even in quiet period and here again dissimilar for Dawn and Dusk? Firstly, the MAGSAT (4/81) model used for base subtraction may not be fully adequate for this purpose. If so, there is nothing one can do about it except wait for a better model. Secondly, it may be that Sq effects are not negligible even at Dusk and Dawn and may even be dissimilar for Dusk and Dawn. Sugiura and Hagan (1979) have already indicated such a possibility. Thirdly, the quiet-time ring current may not be negligible and may have dissimilar effects for Dusk and Dawn. In practice, this effect will be mixed up with the possible Sq dissimiliarity. Fourthly, since every successive pass (Dawn or Dusk) is about 1.6 hours apart, the earth would have turned under the satellite by about 24^0 in longitude. Thus, every pass would be covering a different ground terrain and hence perhaps a different kind of ground anomaly. Thus, a variety of effects could be involved and all these need to be estimated and corrected either individually or collectively. We acheived this in the following way.

We used data for about 1200 Dawn and 1200 Dusk passes which occurred during Nov. 2, 1979 and Jan. 18, 1980. The passes were separated first into 72 longitude groups (longitude of equatorial crossing) viz. -180^0 to -175^0, ... -5^0 to 0^0, 0^0 to $+5^0$, ... $+175^0$ to $+180^0$. For each one of these longitude groups, ΔH_0 (Dusk) and ΔH_0(Dawn) were plotted separately against the corresponding geomagnetic Dst. Fig. 3(a) left half shows ΔH_0 (Dawn) versus Dst, and the right half shows ΔH_0 (Dusk) versus Dst, for the longitude belt 0^0 to $+5^0$. There were about 15 passes involved, of each type. The correlation coefficients are reasonably high, (about +0.80 or more) and the regression lines drawn are for ΔH_0 (Dawn or Dusk) as the independent parameter and Dst as the dependent parameter. In each case, the intercept on the ΔH_0 axis (ordinate) corresponds to Dst = 0 and hence gives us an estimate of the quiet-time base level of ΔH_0 (Dawn or Dusk). For example, for the longitude belt 0^o to $+5^o$, the base value of ΔH_0 (Dawn) is -26 nT and for H_0 (Dusk), it is -40 nT.

Fig. 3(b) shows similar plots for the longitude belt $+5^o$ to $+10^o$. The base levels are now -31 nT for ΔH_0 (Dawn) and -41 nT for ΔH_0 (Dusk).

Similar plots were made for all the other longitude belts. Fig. 4 shows a plot of the base values ($\Delta\overline{H}_0$, $\Delta\overline{Y}_0$, $\Delta\overline{Z}_0$) versus longitude, for ΔH_0 (Dusk) in the first row and ΔH_0 (Dawn) in the second row. Considerable longitude variation is noticed, probably due to varying ground anomaly effects, which are brought out clearly in the third row depicting the <u>average</u> of Dawn and Dusk. The Bangui anomaly at longitudes 0^o to $+20^o$ can be seen. The fourth row depicts the <u>difference</u> (Dusk minus Dawn) and represents Dusk-Dawn asymmetries due to Sq effects (Sugiura and Hagan, 1979), quiet-time ring currents etc. These too seem to be longitude dependent. The other rows in Fig. 4 show similar base levels for the Y and Z components.

Irrespective of the nature of these base levels viz. whether due to Sq effects, ring current effects, ground anomalies etc., it should be enough for our purpose to subtract these from the actual values of ΔH_0 (Dusk) and ΔH_0 (Dawn) of every pass (with due consideration for the longitude belt), so that the residuals so obtained could be considered as depicting true storm effects. Fig. 5 is a reproduction of some parts of Fig. 2, after such a correction (base level subtraction) is applied. Fig. 5(a) refers to Nov. 3-5, 1979 and a comparison with Fig. 2(a) shows that the scatter has reduced considerably and values are now clustered mostly near zero. Fig. 5(b) refers to the storm period Nov. 11-15, 1979 and a comparison with Fig. 2(c) shows a clear-cut hysteresis loop in contrast to the earlier confusion of points. Thus, in the main phase of the storm (Nov.11-13) (full dots and lines), ΔH_o (Dusk) seems to attain negative values numerically almost double of those of ΔH_o (Dawn). Somewhere near the end of the main phase, ΔH_o (Dusk) saturates. The ΔH_o (Dawn) continues to increase (negative) but never catches up with ΔH_o (Dusk). Only after a partial recovery of ΔH_o (Dusk), the ΔH_o (Dawn) catches up with the same and, thereafter, the two recover together.

In the interval of 78 days (Nov. 2, 1979 - Jan. 18, 1980) that we studied, there were two major storms, one during Nov. 11-16, 1979 and another during Jan. 1-3, 1980, besides several minor storms as during Nov. 7-8, Nov. 24-25, Dec. 3-5, Dec. 28-30, 1979 and Jan. 13-14, 1980. In Fig. 5(c) we show a plot of ΔH_o (Dusk) versus ΔH_o (Dawn) for the other major storm of Dec. 31, 1979 - Jan. 3, 1980. There is a hysteresis loop clearly visible, remarkably similar to the loop of Fig. 5(b).

Fig. 6 shows a plot of ΔH_o (Dusk) and ΔH_o Dawn) for the storm of Nov. 11-15, 1979. The top curves (row 1) and the Dst (second row) are the same as those shown in Fig. 1. Rows 3 and 4 show ΔY_o and ΔZ_o. All these are uncorrected for base levels. When the base level corrections are applied, the plots look as shown in rows 5, 6 and 7. Considerable modifications seem to have occurred because of the base level corrections. Fig. 7 shows the plots of base-level-corrected values of ΔH_o, ΔY_o, ΔZ_o for Dawn and Dusk for the storm of Dec. 31, 1979 - Jan. 2, 1980.

The main features of these storms may be summarised as follows:

a) When values corrected for base level are used, both ΔH_o (Dusk) and ΔH_o (Dawn) show values near zero during quiet periods, as expected.

b) When a storm commences as seen by the Dst attaining negative values, the ΔH_o (Dusk) responds first and attains values similar to Dst. The ΔH_o (Dawn) does not seem to respond to small Dst changes. For large Dst (negative) values, ΔH_0 (Dusk) seems to follow suit while ΔH_0 (Dawn) lags behind and never reaches the highest ΔH_0 (Dusk) level. After Dst and ΔH_0 (Dusk) have recovered partially, ΔH_0 (Dawn) catches up with ΔH_0 (Dusk) and thereafter, the two recover together. A plot of ΔH_0 (Dusk) versus ΔH_0 (Dawn) shows a hysteresis type loop, indicating larger and earlier storm effects in the Dusk sector as compared to Dawn sector.

c) During the storm main phase, ΔY_0 (Dusk) and ΔY_0 (Dawn) also show large variations (several nT) and often reverse to each other. Thus,meridional currents are indicated, which could also be due to nonparallelism between the central plane of the ring current and the geographical equatorial plane.

B. Comparison of MAGSAT and ground data

So far, we studied the storm-time variation characteristics at the MAGSAT altitudes only. We now compare these with ground observations. Form WDC-A, Boulder, Colorado, we obtained the hourly values of the H component for several low and mid-latitude locations, as listed in Table 1 according to geographical longitudes. Some of these could be considered as in the same longitude belt. For example, Tsumeb, Bangui and Hermanus have roughly the same longitude (about 15°E). For these locations, there would be one Dawn pass and one Dusk pass per day which could be compared with ground ΔH values at Dawn and Dusk, choosing the proper geographical latitudes on the passes to match with the geographical latitudes of the ground stations as given in Table 1. Since only hourly values near Dusk or Dawn will be used, a possible error of half an hour in time is involved. Also, a pass may not have occurred exactly at a particular ground location longitude; but there will generally exist a pass within $\pm 12^{\circ}$ of the longitude of the location. Thus, inaccuracies of about 1/2 hour in time and about 12° in longitude may be involved. During quiet periods, successive hourly values at Dawn and Dusk do not change by more than a few nT. During disturbed periods, inaccuracies of about ±5 nT could occur.

For Nov. 1979, we omitted data for Nov. 2, as these seemed doubtful. For the 28 days Nov. 3-30, 1979, Fig. 8 shows a plot of ΔH at ground for Bangui (4.6°N, 18.6°) versus ΔH at MAGSAT for passes near 18.6°E longitude (±12°), for Dawn passes in the left half and Dusk passes in the right half. Each graph has 28 points. For ground values, the base is arbitrary. Also, for satellite values, the ΔH is original and no base-level correction is applied; because, for a given longitude, the correction is the same for all values. The purpose of this plot is not to study the intercepts on the axes but to see whether the points lie on a straight line and, if so, to estimate the slopes. For this, a correlation analysis was carried out between the 28 values of ΔH at satellite (for geographical longitude 5°N, appropriate for Bangui) and ΔH at Bangui. The correlation coefficient was high (exceeding +0.9) and the two regression lines ($Y = mX + c$), one with ΔH at satellite as the independent variable and ΔH at ground as the dependent variable and the other vice versa, were very close to each other as can be seen in Fig. 8. Similar analysis was carried out using ΔH at ground for all the other locations. Table 1 lists the values of the correlation coefficients and the slopes. As can be seen, all the correlation coefficients are high (exceeding +0.80). Also, all the slopes are <u>near unity</u>. Since the 28 day interval Nov. 3-30, 1979 had one major storm (Nov. 11-15) and a few minor storms, the range of values was quite large (about 100 nT). In this range, the ground values and satellite values tallied with an accuracy of about 10 nT. Thus, with a probable inaccuracy of about 10%, the storm effects at ground and at MAGSAT altitude seem to be identical and hence mostly of magnetospheric origin. Ionospheric contributions, if any, would be about 10% or less.

At the bottom of Table 1, we give the <u>average</u> values of the slopes. These seem to be slightly higher when ΔH (satellite) is the independent variable. Thus, storm effects at the satellite may be ~ 3% larger than those at ground.

It may be noted that the analysis in Table 1 referred to variations observed at ground and at MAGSAT altitudes. Now, it is known that for any external current system, there is a coresponding induction effect in the conducting earth. A number of investigations using Sq and Dst variations (e.g. Eckhardt et al., 1963; Banks, 1969) suggest a highly conducting layer at depths between 400-600 Km. Hermance (1982) mentions that for MAGSAT altitudes, the effect of a conducting mantle at a depth of 400 Km would be an induced contribution of about 35% of the external field. At the surface of the earth, it would be about 40%. Thus, if the external ring current has an effective field of say 100 nT, the MAGSAT will record it as 100 + 35 = 135 nT while the ground locations would record it as 100 + 40 = 140 nT. Thus, MAGSAT response is expected to be about 3-4% lesser than the ground response, if the source field is in the magnetosphere. If, however, even a part of the source is in the ionosphere, the effect would be a partial cancelling of the external and internal field for MAGSAT altitudes. Thus, the response at MAGSAT would be much lesser than that at ground. Thus, in both these cases, one expects the MAGSAT response at least a few percent lesser than at ground. Now, in Table 1, the average slopes when the Satellite values form the independent variable are 0.95 for Dawn and 0.97 for Dusk. This slight reduction from unity (about 3-5%) could be interpreted as an indication of a lesser response at MAGSAT as compared to ground. However, in that case, the result of the reverse correlation analysis, when the ground values are the independent variable, should show slopes greater than unity. This did not turn out to be the case, as the average slopes for this case seem to be 0.91 for Dawn and 0.93 for Dusk (see Table 1). Now, in a correlation analysis, the general tendency is for the slopes to be lesser, in favour of the abscissa, unless the correlation coefficient is unity. Thus, all these values could be interpreted as being almost unity. But, amongst these, there is certainly no indication that the satellite values are smaller than ground values. If anything, comparison of the numbers 0.95, 0.97 on one side and 0.91, 0.93 on the other, makes one conclude that the first group is larger by about 3-5% and thus, the satellite values are larger by about this amount.

Taken on its face value, we do not understand this result. However, the scatter of points in Fig. 8 is rather large and we believe that the accuracy of this analysis is not good enough to judge differences of the order of a few percent. Hence, all that we claim is that ground and MAGSAT responses are the same within an accuracy of about 10%. In any case, the evidence for ionospheric effects is almost nonexistent, for Dawn and Dusk hours.

It is interesting to note that Araki et al. (1982), who studied the occurrence of SSC at MAGSAT, found that for one event, the SSC at 0738 UT on Nov. 30, 1979 (only a minor storm) did have some contribution from ionospheric sources. Thus, ionospheric contributions at Dusk & Dawn may be occurring either very infrequently, or probably are too small to be detected in an analysis of hourly values.

C. <u>Latitudinal variation of storm effects</u>

During storm periods, ΔH_0 is large negative. We now explore the latitudinal variation of ΔH during storms.

Figure 9(a) shows the latitudinal variation of ΔH for the Dusk pass No. 184 which occurred on Nov. 13, 1979 at about 2300 UT at an equatorial longitude of about -79^0 i.e. 79^0W. On its face value, there seems to be a significant latitude dependence, with the largest storm effects (ΔH = -140nT) at about 15^0S latitude. However, it is necessary to check that such a minimum at -15^0 is not a permanent feature in this longitude zone. For studying this, the average latitudinal variation of ΔH for six quiet day Dusk passes (Dst within ±10nT), which occurred in the longitude belt 75^0-80^0W during the period Nov. 1979 - Jan. 1980, was evaluated. Figure 9(b) shows this average. As can be seen, the minimum at 15^0S <u>is</u> an average quiet-day feature for this longitude zone, probably due to ground anomaly effects. The real storm-time latitude dependence of ΔH would be obtained by subtracting 9(b) from 9(a). The difference is shown in Figure 9(c). Now, the latitudinal distribution is almost flat.

It was obvious, therefore, that, to study the correct latitudinal distribution, it was necessary first to establish quiet time patterns like Figure 9(b). This was done for 72 longitude belts, each of 5^{o} width. Figure 10 shows the latitudinal variation of ΔH for longitude belts 0 to $+5^{o}$, $+5^{o}$ to $+10^{o}$, ... $+85^{o}$ to $+90^{o}$. As can be seen, considerable variations are observed, many of which are common to Dusk and Dawn and hence must be due to ground anomalies. However, there are some differences too, indicating that the Sq effects at Dusk and Dawn are not alike. Figure 11 shows similar plots for the Y component. Here, a curious fact is noticed. The Dawn plots show very little latitudinal variations but the Dusk plots show large variations. The vertical arrows indicate the position of the dip equator. As can be seen, ΔY (Dusk) shows a clear transition symmetric about the dip equator. Maeda et al. (1982) have showed this effect from the MAGSAT data and have commented that the D(i.e. Y) variation appears everyday on the low-latitude dusk side and is antisymmetric about the dip equator. They have interpreted this as indicative of meridional current systems in the equatorial ionosphere and associate these with the equatorial electrojet as envisaged in the Untiedt (1967) and Sugiura and Poros (1969) models. We have noticed, however, that these changes are very large in the Y component only and hence, probably indicate the usual Sq pattern of roughly circular currents which, in low latitudes near midday, are mostly east-west but which, at dawn or dusk, are mostly north-south. In the equatorial region, longitudinal differences could arise from the excursions of the Sq currents of one hemisphere into the other (Hutton 1967 a, b) and/or due to solsticial Sq currents through the magnetosphere (Van Sabben, 1970). Since the present investigation is not directly related to the quiet-time variations (Sq or quiet-time ring current), we will not discuss this matter any furthur here but we will use these quiet-time patterns as base levels for subtracting from the disturbed day patterns. The actual values of these base levels are available in tabular form in the MAGSAT reports.

As shown in Figure 1, the period Nov. 11-15, 1979 was a storm period. On Nov. 13, the Dusk pass 170 at about 0100 UT was only moderately disturbed (Dst = -17). However, the successive passes 171, 172 etc. were highly disturbed. All these occurred at different longitudes. From each of these passes, we subtracted the quiet-time latitudinal pattern appropriate to its longitude. The residual patterns so corrected are shown in Figure 12. The dots and full lines refer to ΔH and the crosses and dashes refer to ΔX. The left half shows consecutive Dusk passes 170-181. In the right half, the upper half shows Dusk passes 182-188. The vertical arrows indicate the position of the dip equator. The pass number, Dst and longitude of equatorial crossing are marked for each pass.

It seems from Figure 12 that the ΔH and ΔX variations are very similar to each other, and these are not always symmetric about the geographical or dip equator. In the early stage of the storm (passes 170-177), the northern hemisphere shows larger storm effects. By about pass 178, the pattern is roughly symmetrical. For later passes, the southern hemisphere has larger storm effects. Thus, during the course of the storm, there was a considerable north-south asymmetry of a variable nature. In the case of the present storm, the early part of the storm exhibited stronger storm effects in the northern hemisphere. However, as shown in the lower right half of Figure 12 for the successive disturbed day Dusk passes 936-939, which occurred on Jan. 1, 1980 at about 1800-2200 UT, the storm effect seems to be stronger in the southern hemisphere.

In the middle of the right half of Figure 12, we show a similar plot for the disturbed day Dawn pass 184. In contrast to the Dusk pass 184, the Dawn pass shows a very erratic latitudinal distribution. There is no semblance of a maximum storm effect either at geographic or at dip equator. Instead, one notices maximum storm effects at about ±15^{0} geographical latitudes. We examined some other disturbed-day Dawn passes and noticed largely variable patterns, different for different passes.

Figure 13 shows similar plots for the Y component. Here, symmetry about the geographic or the dip equator (vertical arrows) seems to be more an exception than a rule. In general, the Y variation is erratic, with no systematic variation from one pass to the next. To us, it seems that these variable patterns of ΔX and ΔY storm-time variations may be related to latitudinal meanderings of the central plane of the magnetospheric storm-time ring current and/or complications due to field-aligned currents, different in different local time zones (Dawn or Dusk).

Figure 14 shows the latitudinal patterns of ΔX and ΔY averaged for all the storm-time passes 170-188. The upper half has geographic latitude as abscissa. ΔX shows a maximum storm effect (largest negative values) near the geographic equator (at about 5^{o}S) with roughly a cos θ dependence on either side. However, ΔY does not show any such effect clearly. Instead, one observes a minimum storm effect (smallest negative values) at about -10^{o} i.e. 10^{o}S. Thus, on the average, the central plane of the storm-time ring current is almost coincident with the geographic equatorial plane, with a probable shift slightly southwards.

The lower half of Figure 14 shows similar average latitudinal patterns for ΔX and ΔY with dip latitude as abscissa. No clear latitude dependence is noticed, for either ΔX or ΔY. Thus, the storm-time ring current does not seem to be influenced by the dip equator.

These results are in general agreement with our earlier published results (Kane and Trivedi, 1981), about the central plane of the ring current.

4. Summary and Conclusions

The results of the present investigation may be summarized as follows:

(i) From the values of X, Y, Z as given in the Investigator B tapes, H was calculated as $H = (X^2 + Y^2)^{1/2}$. The tapes also gave model values of X, Y, Z. viz. XMD YMD, ZMD for MAGSAT (4/81). From these, HMD was calculated as $HMD=(XMD^2+YMD^2)^{1/2}$. The residuals $\Delta H = H - HMD$, $\Delta X = X - XMD$, $\Delta Y = Y - YMD$, $\Delta Z = Z - ZMD$ were obtained and used for analysis.

(ii) ΔH_0, i.e. the value of ΔH at equatorial crossing, showed that ΔH_0 (Dusk) and ΔH_0 (Dawn) were always non-zero, mostly negative. In general, ΔH_0 (Dusk) was more negative than ΔH_0 (Dawn), even on quiet-day passes.

(iii) From a correlation analysis of ΔH_0 (Dusk) and ΔH_0 (Dawn) versus Dst, the quiet-time (Dst = 0) base levels of ΔH_0 (Dusk) and ΔH_0 (Dawn) were estimated for 5^0 longitude belts. These base-levels were subtracted from the original values. The residuals of ΔH (Dusk), ΔH (Dawn), ΔY (Dusk), ΔY (Dawn) ΔZ (Dusk), ΔZ (Dawn) so obtained showed that:

(a) On quiet days, ΔH (Dusk) and ΔH (Dawn) residuals were now almost zero, as expected.

(b) During the storm of Nov. 11-15, 1979, Dst started increasing (negative) at about 0200 UT on Nov. 13. ΔH_0 (Dusk) started increasing (negative) too and followed Dst almost faithfully. However, ΔH_0 (Dawn) started increasing (negative) somewhat later and never reached the highest level attained by ΔH_0 (Dusk). When ΔH_0 (Dusk) started recovering, ΔH_0 (Dawn) caught up with the same. Thus, ΔH_0 (Dusk) showed more intense storm effects, occurring earlier than ΔH_0 (Dawn). A sort of hysteresis loop was noticed. Another storm of Dec. 31, 1979 - Jan. 2, 1980 showed a similar behaviour.

(c) During the storm main phase, ΔY_0 (Dawn) and ΔY_0 (Dusk) showed large variations. Thus, some meridional currents were indicated. Noncoincidence of the central plane of the ring current with the geographic equatorial plane is also a possibility.

(d) ΔZ_0 changes were small.

(iv) Using the hourly values of 16 ground locations, at different latitudes and longitudes in the low and mid-latitude region, a comparison was made of ΔH at ground near Dawn and Dusk (separately) and ΔH at MGASAT altitudes, for the latitude and longitude appropriate for the ground location. Excellent correlations were obtained with slopes almost unity. Thus, within a possible error of about 10%, the storm effects at MAGSAT altitudes were found to be the same as at ground, indicating predominantly a magnetospheric origin. Ionospheric effects, if any, should be 10% or less, both for Dawn as well as Dusk. However, ionospheric effects may be there at other local times (e.g. midday) which are not possible of investigation with MAGSAT data. Also, small ionospheric effects could probably be detected by studying data finer than the hourly values used by us.

(v) To study the latitude dependence of ΔH, ΔX, ΔY during storms, the quiet-day latitudinal patterns of these parameters were obtained by averaging for all quiet-day (Dst within ±10 nT) passes which occurred during Nov. 2, 1979 - Jan. 18, 1980, separately for Dawn and Dusk, separately for 72 longitude belts of 5^o width. These quiet-day average patterns were subtracted from the individual storm-time passes with due regard to the appropriate longitudes. The storm-time passes so corrected indicated the following:

(a) For the storm of Nov. 13-14, 1979, the latitudinal distribution of ΔH (which was the same as for ΔX), was not symmetrical either about the geographic equator or the dip equator. Instead, in the initial part of the storm main phase, the storm effect was larger in the southern hemisphere and later, it became larger in the northern hemisphere. In the storm of Dec. 31, 1979 - Jan. 2, 1980, the pattern was probably reverse. Thus, variable north--south asymmetry seems to be a prominent feature of the storm-time ring current.

(b) When the average for several consecutive storm-time passes was obtained, the latitudinal distribution looked roughly symmetric about the geographic equator with a possible cos Θ dependence. No such relationship with dip equator was obtained.

(c) The Y component did not show any symmetry about the geographic or dip equator nor any consistent latitudinal distribution from pass to pass. Variations were large but erratic during the main phase of the storm.

(vi) From these variations, it seems that the central plane of the storm-time ring current does not remain steady during the course of the storm, but shows latitudinal meanderings, variable north-south asymmetries and probably non-confinement to the geographic equatorial plane. Complications like field-aligned currents connecting equatorial magnetosphere to auroral ionosphere seem to be present, different for Dawn and Dusk sectors. However, in the low latitude region for both Dusk as well as Dawn hours, the storm effect seems to be mostly (about 90%) above the MAGSAT altitudes and hence not in the ionosphere.

The average characteristics of storm-time geomagnetic variations were studied in detail by Sugiura and Chapman (1960), who showed that, superimposed upon the isotropic, world-wide Dst, there was a disturbance local-time inequality DS which has a sinusoidal variation with a maximum in the morning (dawn) sector and a minimum in the evening (dusk) sector. Thus, the net effect would be to hamper the negative Dst change in the morning and to accentuate Dst in the evening. In our analysis, ΔH_0 (Dusk) is always greater (negative) than ΔH_0 (Dawn), which seems to agree with the above average picture. However, the hysteresis effect we observed indicates more complexities in the Dusk-Dawn asymmetry, probably due to field-aligned currents as envisaged in the model of Kamide and Fukushima (1972). The MAGSAT data are restricted to the Dawn and Dusk sectors and hence give only a glimpse of the local time DS effect. It is hoped that future programs would yield a more comprehensive look at this problem. What MAGSAT has yielded is certainly enough to warrant an attempt at a more elaborate program.

Acknowledgements

Thanks are due to the MAGSAT teams for the successful mission and for supplying us the data for carrying out the MAGSAT Project M55, and to Dr. Langel for useful discussions. Thanks are due to WDC-A, Boulder, Colorado for the ground magnetic data. Thanks are due to Dr. Nelson de Jesus Parada, INPE General Director for support. This work was partially supported by FNDCT, Brazil under contract FINEP-537/CT.

Captions for Figures

Figure 1 - Plots of ΔH_0 i.e. ΔH = H'(observed) minus H (Model) for equatorial crossings, for DUSK (crosses and dashes) and DAWN (dots and full lines) as also of Dst, for Nov. 2-7, 1979 (top), Nov. 8-13, 1979 (middle) and Nov. 14-19, 1979 (bottom). Kp is also indicated as histograms.

Figure 2 - ΔH_0 (Dusk) versus ΔH_0 (Dawn) for:

(a) Nov. 3-5, 1979,

(b) Nov. 7-10, 1979 (crosses show doubtful Dusk values),

(c) Nov. 11-15, 1979 (storm period, crosses represent recovery period Nov. 14-15, 1979),

(d) Nov. 16-20, 1979.

Regression lines and correlation coefficients γ are indicated.

Figure 3 - ΔH_0 (Dawn) versus Dst (left half) and ΔH_0 (Dusk) versus Dst (right half) for the 5^o longitude belts (a) Longitude 0^o to $+5^o$ and (b) Longitude $+5^o$ to $+10^o$. The correlation coefficients γ and the regression lines are indicated. Circled numbers indicate values (nT) of intercepts on the ΔH_0 axis and represent the base values for these two longitude groups.

Figure 4 - Longitude distribution of the base values $\Delta\overline{H}_0$, $\Delta\overline{Y}_0$, $\Delta\overline{Z}_0$ for Dawn and Dusk, the average AVER=(Dusk + Dawn)/2 and, the difference DIFF = (Dusk - Dawn). Negative values are shown shaded.

Figure 5 - ΔH_0 (Dusk) versus ΔH_0 (Dawn) using base-corrected values for,

(a) Nov. 3-5, 1979,

(b) Nov. 11-15, 1979 (storm period, crosses refer to recovery Nov. 14-15),

(c) Dec.31, 1979-Jan. 3, 1980 (storm period, crosses refer to recovery Jan. 2-3)

Figure 6 - Plots for the storm period Nov. 11-15, 1979 for Dawn (dots and full lines) and Dusk (dashes and crosses)

Row 1 - ΔH_0 (Dusk) and ΔH_0 (Dawn) uncorrected
Row 2 - Geomagnetic Dst
Row 3 - ΔY_0 (Dusk) and ΔY_0 (Dawn) uncorrected
Row 4 - ΔZ_0 (Dusk) and ΔZ_0 (Dawn) uncorrected
Row 5 - ΔH_0 (Dusk and Dawn) corrected for base levels
Row 6 - ΔY_0 (Dusk and Dawn) corrected for base levels
Row 7 - ΔZ_0 (Dusk and Dawn) corrected for base levels.

Figure 7 - Plots of Dst and the base-level-corrected values of ΔH_0, ΔY_0, ΔZ_0 for Dawn (dots and full lines) and Dusk (dashes and crosses), for the storm period Dec.31, 1979 - Jan. 2, 1980.

Figure 8 - ΔH at Bangui (5^oN, 19^oE) versus MAGSAT ΔH values at 5^oN for Dawn and Dusk passes near 19^oE longitude, for Nov. 3-30, 1979. Excellent correlations with regression lines of slope almost unity are indicated, implying very good parallelism between ground variations and MAGSAT variations.

Figure 9 - Latitudinal variation of ΔH for:

(a) The specific disturbed day Dusk Pass No. 184 at a longitude of about -79^o.
(b) Quiet-day base level obtained as average of six quiet day passes in the longitude belt 75^o-80^oW.
(c) The difference (a) minus (b).

Figure 10 - Average latitudinal variations for ΔH (Dusk) (left half) and ΔH(Dawn) (right half) for successive 5^o longitude belts in the longitude range 0^o to $+90^o$. + = East, - = West.

Figure 11 - Average latitudinal variations for ΔY (Dusk) (left half) and ΔY (Dawn) (right half) for successive 5° longitude belts in the longitude range 0 to $+90^{\circ}$. Vertical arrows indicate the position of the dip equator.

Figure 12 - Latitudinal variation of ΔH (dots and full lines) and ΔX (crosses and dashes), both corrected for base levels, for the Dusk passes Nos. 170-188, during the storm of Nov.11-15, 1979, as also for the Dawn Pass No. 184 and for the Dusk passes Nos. 936-939 in Jan. 1980. The pass number, longitude and Dst are indicated for each pass. Vertical arrows indicate the position of the dip equator.

Figure 13 - Same as Fig. 12, but for ΔY.

Figure 14 - Average latitudinal distribution of ΔX and ΔY for the storm-time Dusk passes Nos. 170-188 on Nov. 13-14, 1979.
Upper half: For geographical latitudes.
Lower half: For dip latitudes.

<u>Captions Table</u>

Table 1 - List and details of stations and results (correlation coefficients and slopes with errors) of a correlation analysis for a linear fit $Y = mX + c$, where Y = Independent variable, X = Dependent variable, m = slope.

References

Akasofu S.I. and Chapman S., "Solar-Terrestrial Physics", Clarendon Press, Oxford (1972).

Araki T., Iyemori T., Tsunomura S., Kamei T. and Maeda H., Detection of an ionospheric current for the preliminary impulse of the geomagnetic sudden commencement. Geophys. Res. Letters, 9, 341-344 (1982).

Banks R.J. Geomagnetic variations and the electrical conductivity of the Upper mantle, Geophys. J., 17, 457-487 (1969)

Cahill L.J. Inflation of the inner magnetosphere during a magnetic storm. J. Geophys. Res., 71, 4505-4519 (1966).

Chapman S. and Bartels J. "Geomagnetism" Vol. I and II Oxford Univ. Press, Oxford (1940).

Eckhardt, D.H., Larner K. and Madden T.R., Long period magnetic fluctuations and mantle conductivity estimates. J. Geophys. Res., 68, 6279-6286 (1963)

Hermance J.F. Model simulations of possible electromagnetic induction effects at MAGSAT activities. Geophys Res. Letters, 9, 373-376 (1982)

Hutton R. Sq currents in the American equatorial zone during the IGY-I. Seasonal effects. J. Atmos. Terr. Phys., 29, 1411-1427 (1967a).

Hutton R. Sq currents in the American equatorial zone during the IGY-II. Day-to-day Variability. J. Atmos. Terr. Phys., 29, 1429-1442 (1967b).

Kamide Y. and Fukushima N., Positive geomagnetic bays in evening high latitudes and their possible connection with partial current. Rep. Iono. Space Res. (Japan). 26, 79-101 (1972).

Kane R.P. Characteristics of storm-time geomagnetic daily variation J. Atmos. Terr. Phys., 33, 1585-1595 (1971).

Kane R.P. Dependence of the daily ranges of geomagnetic variations on Ap. J. Atmos. Terr. Phys., 34, 1105-1117 (1972)

Kane R.P. Global evolution of the DS component during geomagnetic storms. J. Geophys. Res., 78, 5585-5595 (1973).

Kane R.P. Evolution of disturbance daily variation DS and interplanetary plasma parameters. Proc. Ind. Acad. Sci. 80A, 124-139 (1974)

Kane R.P. and Trived N.B. Central plane of the ring current responsible for geomagnetic disturbance in the South-American region. Annals de Geophys., 37, 271-280 (1981).

Langel R.A. and Cain J.C. OGO-2 magnetic field observations during the magnetic storm of March 13-15, 1966. Annals Geophys., 24, 857-869 (1968).

Maeda H., Iyemori T., Araki T. and Kamei T., New evidence of a meridional current system in the equatorial ionosphere. Geophys. Res. Letters., 9, 337-340 (1982).

Matsushita S. and Campbell W.H. "Physics of the Geomagnetic Phenomena" Vols I and II, Academic Press. New York and London (1967).

Sugiura M. and Chapman S. The average morphology of geomagnetic storms with sudden commencement. Abh. Akad. Wiss. Gottingen Maths-Phys. Klasse. Sonderhaft, Nr. 4. 1-53 (1960).

Sugiura M. and Hagan M.P. Geomagnetic Sq variation at satellite altitudes: Is Sq correction important in MAGSAT data analysis? Geophys. Res. Letters., 6, 397-400 (1979).

Sugiura M. and Poros D.J. An improved model equatorial electrojet with a meridional current system. J. Geophys. Res., 74, 4025-4034 (1969).

Sugiura M. and Poros D.J. Hourly values of equatorial Dst for the years 1957 to 1970. GSFC Publi. X-645-71-278, July (1971).

Untiedt J. A model of the equatorial electrojet involving meridional currents. J. Geophys. Res., 72, 5799-5810 (1967).

Van Sabben D. Solstitial Sq-currents through the magnetosphere. J. Atmos. Terr. Phys., 32, 1331-1336 (1970).

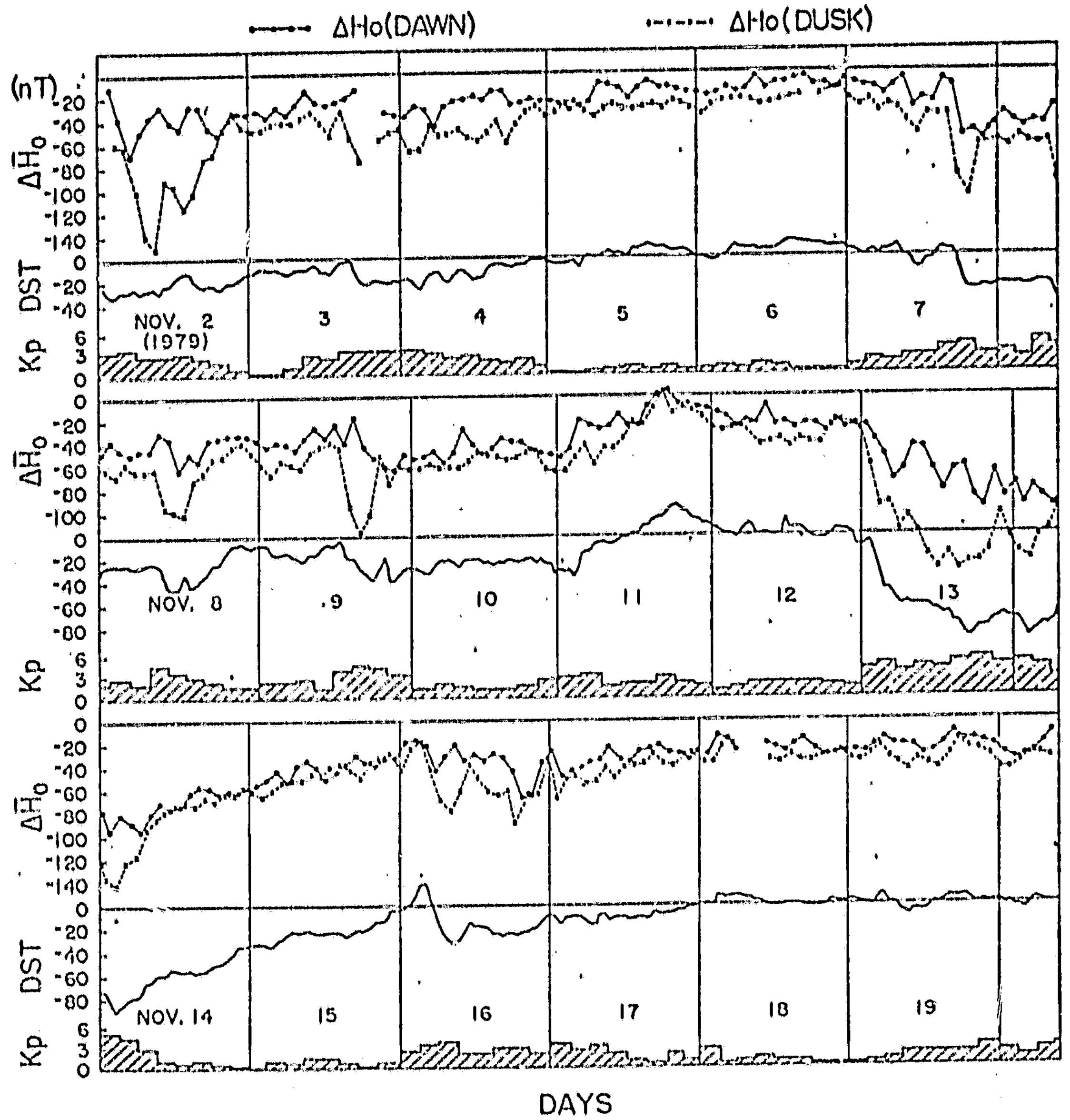
ΔHo(DAWN)
ΔHo(DUSK)
(nT)
$\Delta\bar{H}_o$
DST
Kp
NOV. 2 (1979)
3
4
5
6
7
NOV. 8
9
10
11
12
13
NOV. 14
15
16
17
18
19
DAYS

Fig. 1

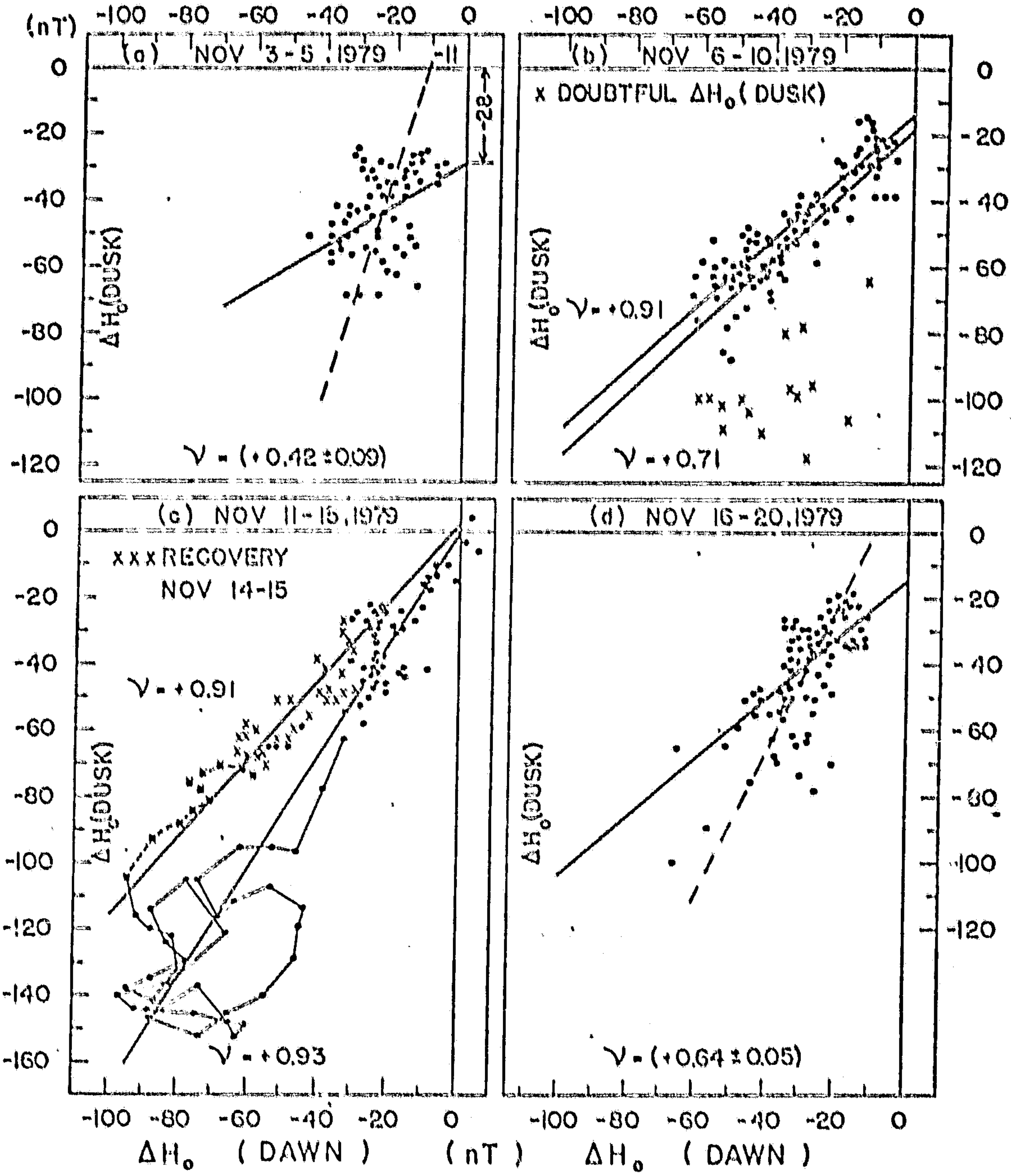
(nT)
(a) NOV 3-5, 1979
-11
-28
ν = (+0.42 ± 0.09)
ΔH₀(DUSK)
(b) NOV 6-10, 1979
x DOUBTFUL ΔH₀(DUSK)
ν = +0.91
ν = +0.71
(c) NOV 11-15, 1979
xxx RECOVERY
NOV 14-15
ν = +0.91
ν = +0.93
(d) NOV 16-20, 1979
ν = (+0.64 ± 0.05)
ΔH₀ (DAWN) (nT) ΔH₀ (DAWN)

Fig. 2

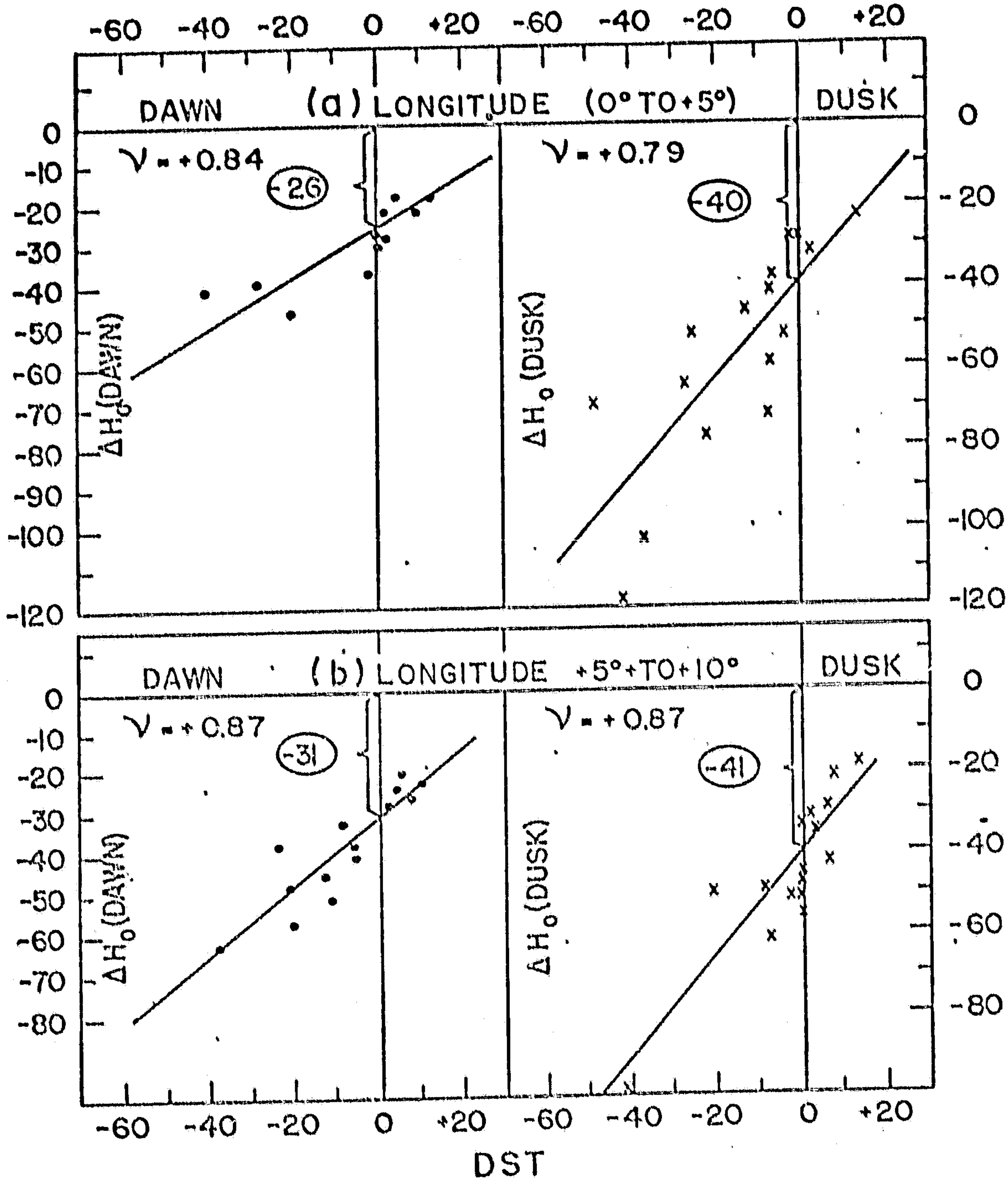
DAWN
(a) LONGITUDE (0° TO +5°)
DUSK
ν = +0.84
-26
ν = +0.79
-40
ΔH₀(DAWN)
ΔH₀(DUSK)
DAWN
(b) LONGITUDE +5° TO +10°
DUSK
ν = +0.87
-31
ν = +0.87
-41
DST

Fig. 3

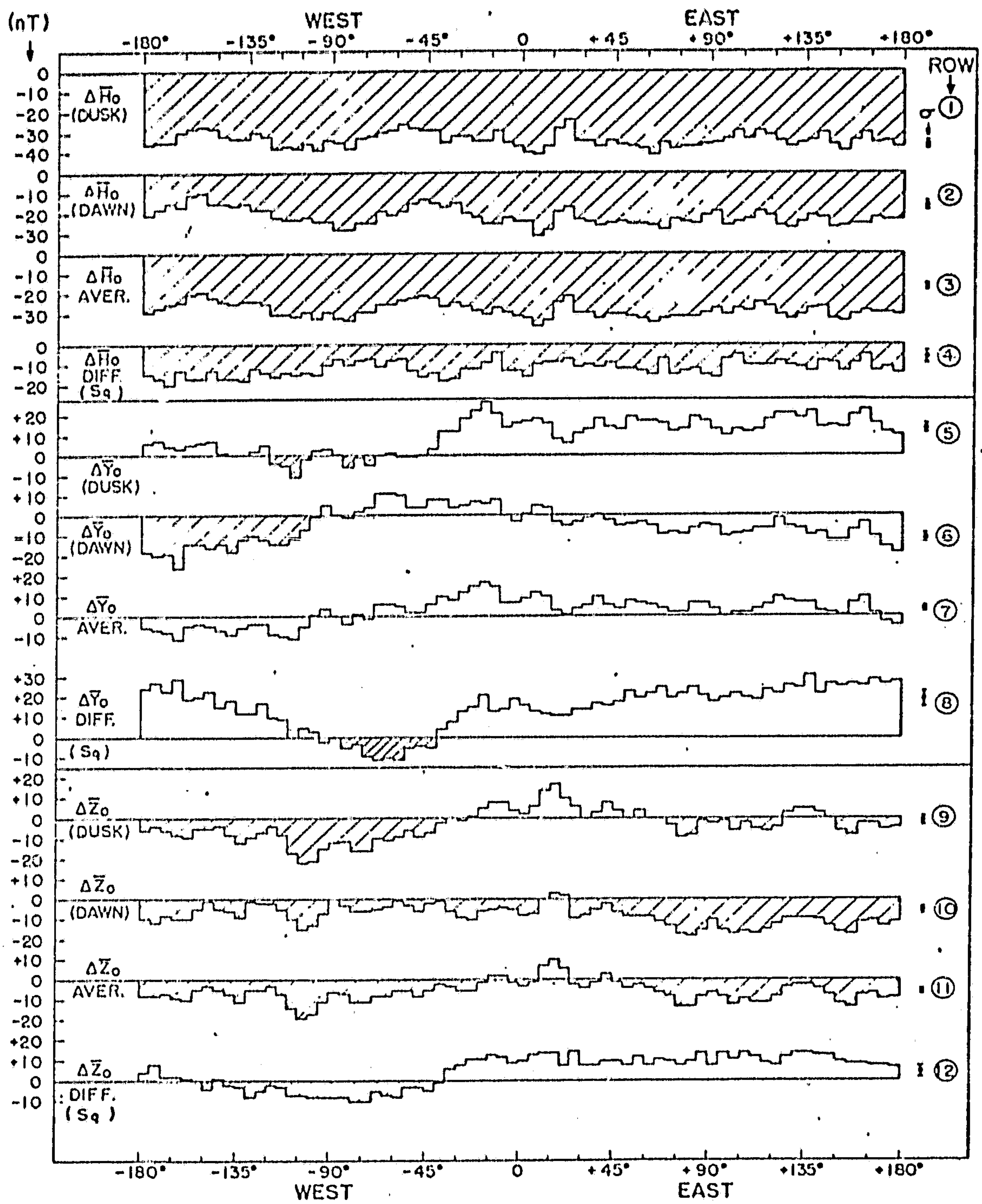
(nT)
WEST
EAST
-180°
-135°
-90°
-45°
0
+45
+90°
+135°
+180°
ROW
$\Delta\bar{H}_o$ (DUSK)
$\Delta\bar{H}_o$ (DAWN)
$\Delta\bar{H}_o$ AVER.
$\Delta\bar{H}_o$ DIFF. (Sq)
$\Delta\bar{Y}_o$ (DUSK)
$\Delta\bar{Y}_o$ (DAWN)
$\Delta\bar{Y}_o$ AVER.
$\Delta\bar{Y}_o$ DIFF. (Sq)
$\Delta\bar{Z}_o$ (DUSK)
$\Delta\bar{Z}_o$ (DAWN)
$\Delta\bar{Z}_o$ AVER.
$\Delta\bar{Z}_o$ DIFF. (Sq)
σ
WEST
EAST
GEOGRAPHIC LONGITUDE

Fig. 4

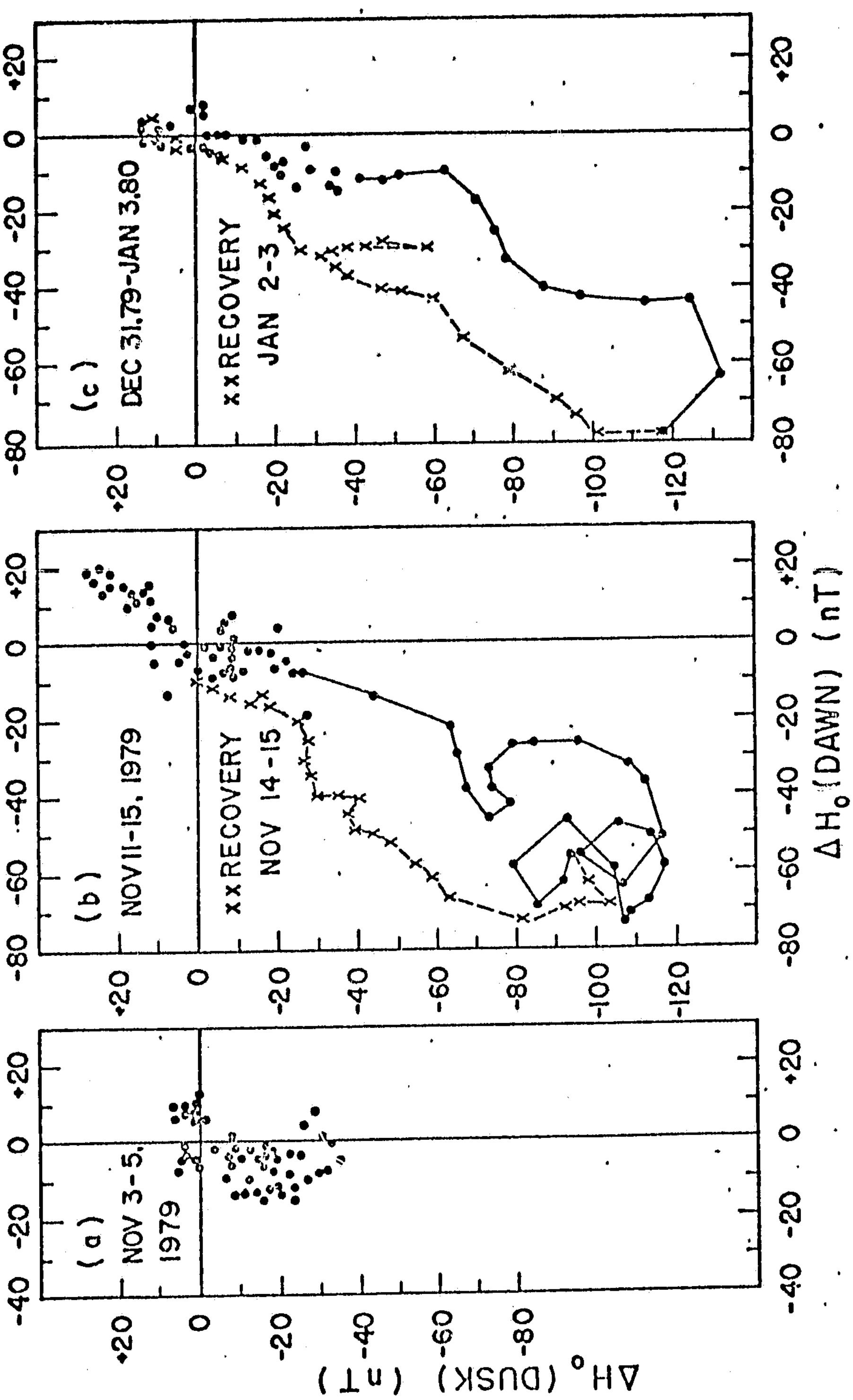
(a) NOV 3-5, 1979
(b) NOV 11-15, 1979
x x RECOVERY NOV 14-15
(c) DEC 31,79-JAN 3,80
x x RECOVERY JAN 2-3
ΔH_o (DAWN) (nT)
ΔH_o (DUSK) (nT)

Fig. 5

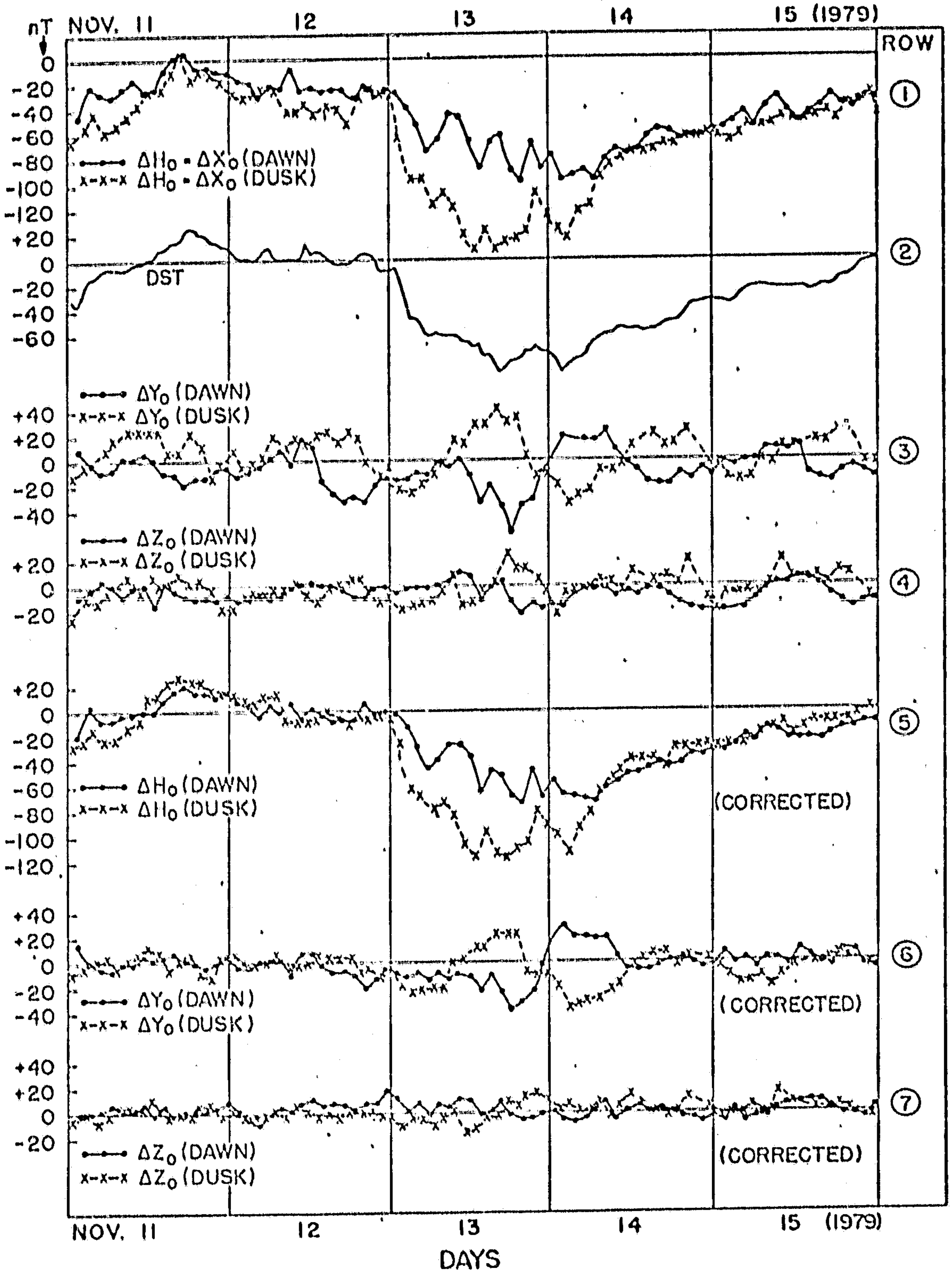
nT
NOV. 11
12
13
14
15 (1979)
ROW
0
-20
-40
-60
-80
-100
-120
+20
0
-20
-40
-60
+40
+20
0
-20
-40
+20
0
-20
+20
0
-20
-40
-60
-80
-100
-120
+40
+20
0
-20
-40
+40
+20
0
-20
①
②
③
④
⑤
⑥
⑦
ΔH₀ ≈ ΔX₀ (DAWN)
ΔH₀ ≈ ΔX₀ (DUSK)
DST
ΔY₀ (DAWN)
ΔY₀ (DUSK)
ΔZ₀ (DAWN)
ΔZ₀ (DUSK)
ΔH₀ (DAWN)
ΔH₀ (DUSK)
(CORRECTED)
ΔY₀ (DAWN)
ΔY₀ (DUSK)
(CORRECTED)
ΔZ₀ (DAWN)
ΔZ₀ (DUSK)
(CORRECTED)
NOV. 11
12
13
14
15 (1979)
DAYS

Fig. 6

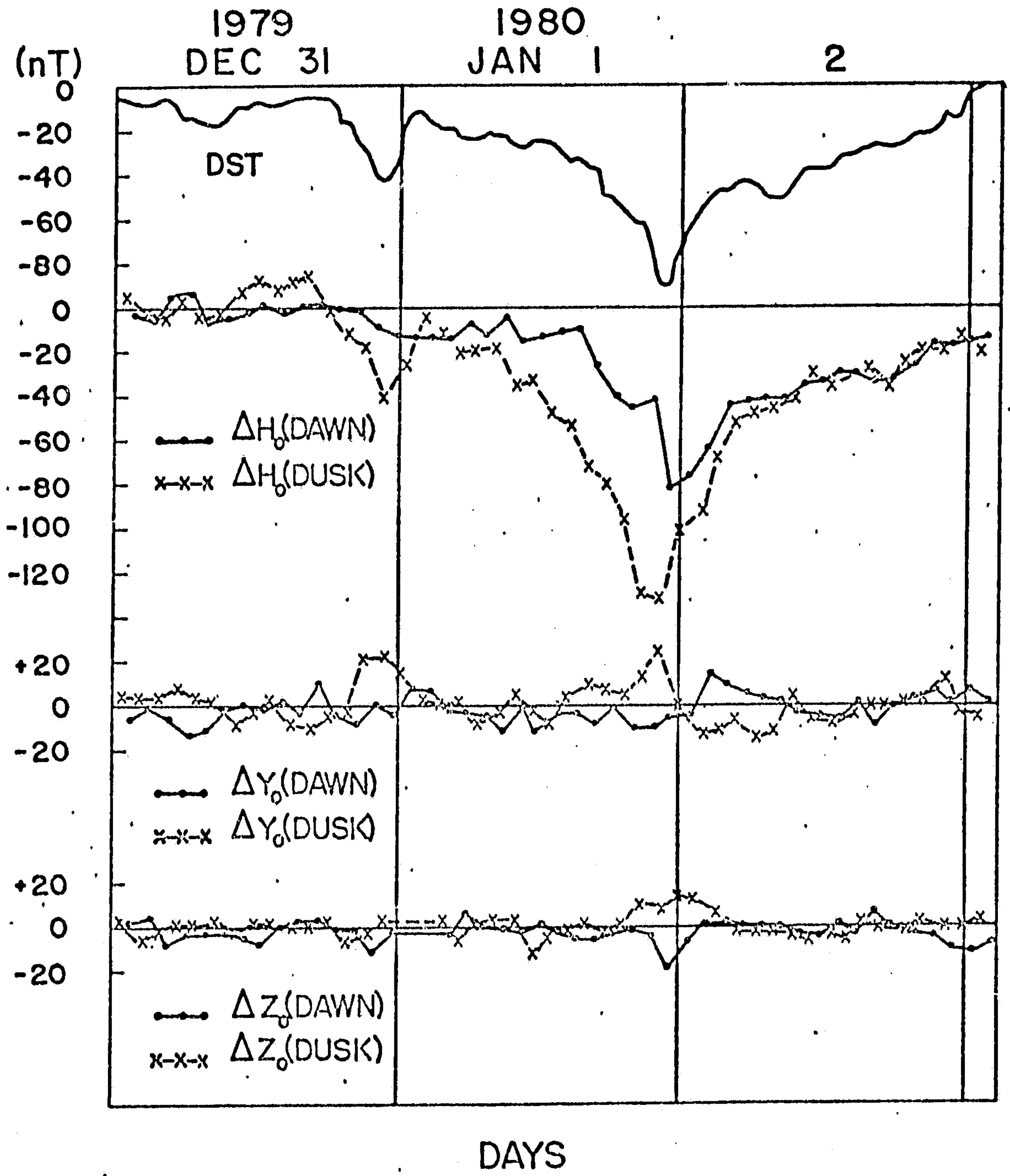
1979
DEC 31
1980
JAN 1
2
(nT)
0
-20
-40
-60
-80
DST
0
-20
-40
-60
-80
-100
-120
ΔH0(DAWN)
ΔH0(DUSK)
+20
0
-20
ΔY0(DAWN)
ΔY0(DUSK)
+20
0
-20
ΔZ0(DAWN)
ΔZ0(DUSK)
DAYS

Fig. 7

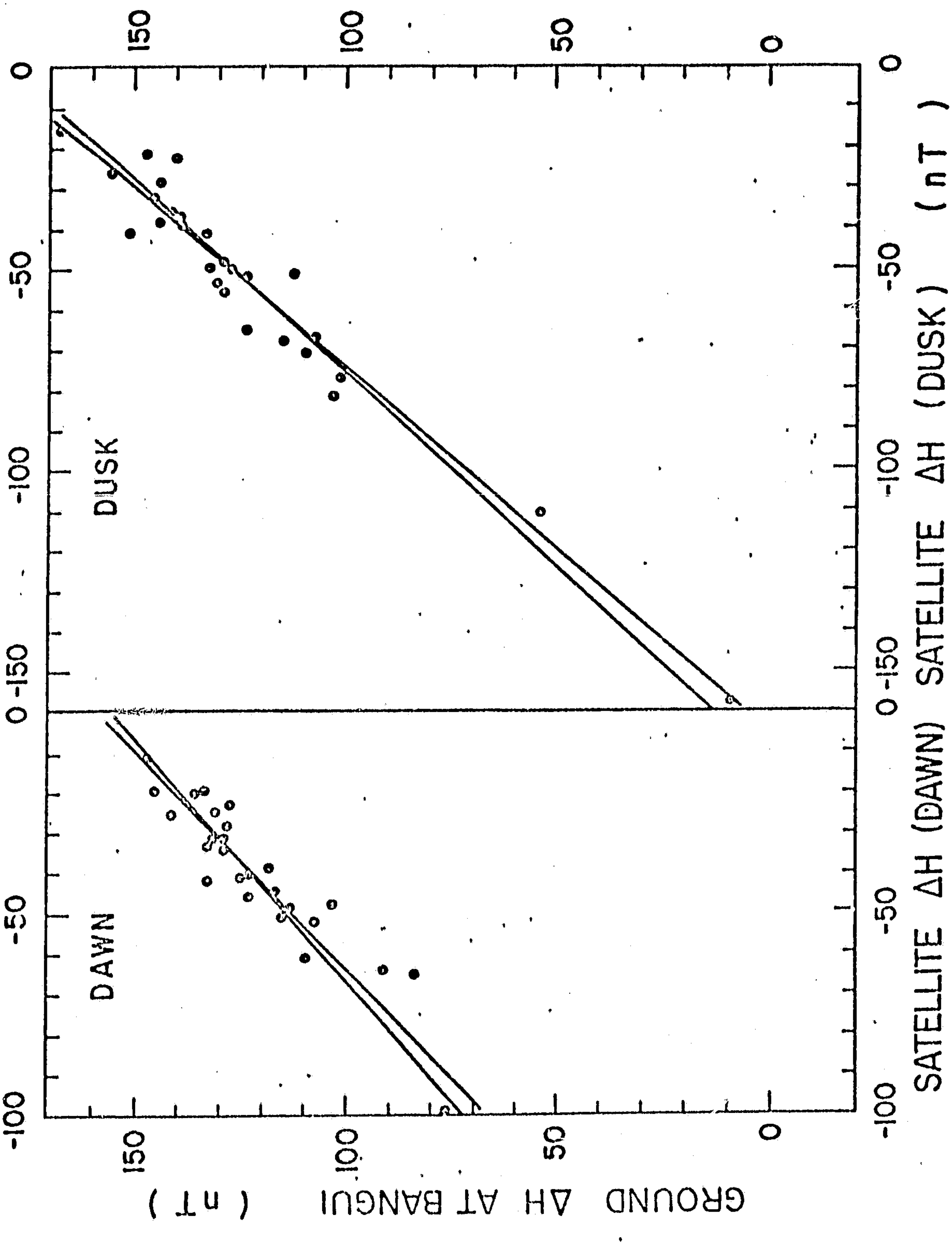
DUSK
DAWN
SATELLITE ΔH (DUSK) (nT)
SATELLITE ΔH (DAWN)
GROUND ΔH AT BANGUI (nT)

Fig. 8

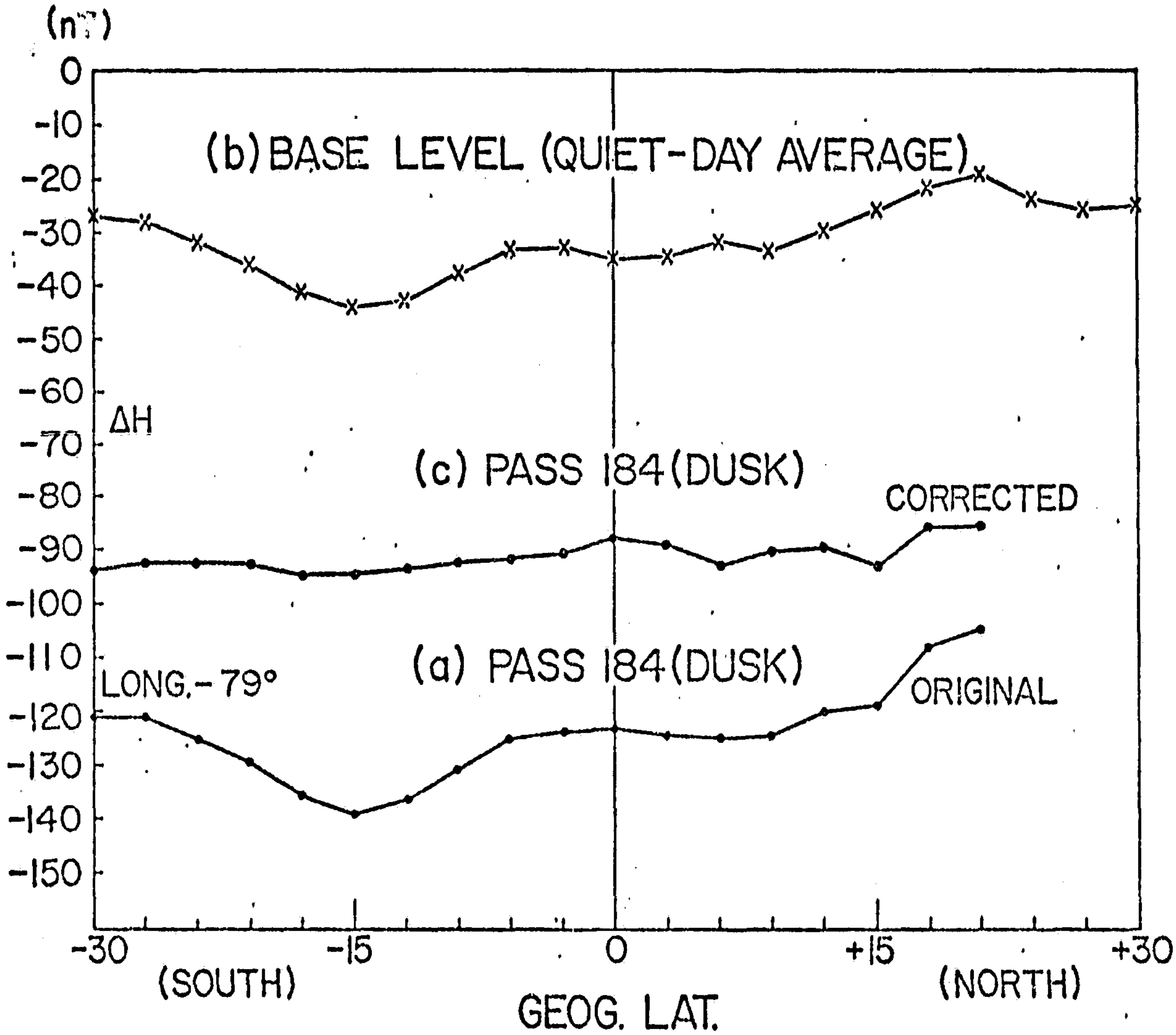
(nT)
0
-10
-20
-30
-40
-50
-60
-70
-80
-90
-100
-110
-120
-130
-140
-150
(b) BASE LEVEL (QUIET-DAY AVERAGE)
ΔH
(c) PASS 184 (DUSK)
CORRECTED
(a) PASS 184 (DUSK)
LONG. - 79°
ORIGINAL
-30
-15
0
+15
+30
(SOUTH)
(NORTH)
GEOG. LAT.

Fig. 9

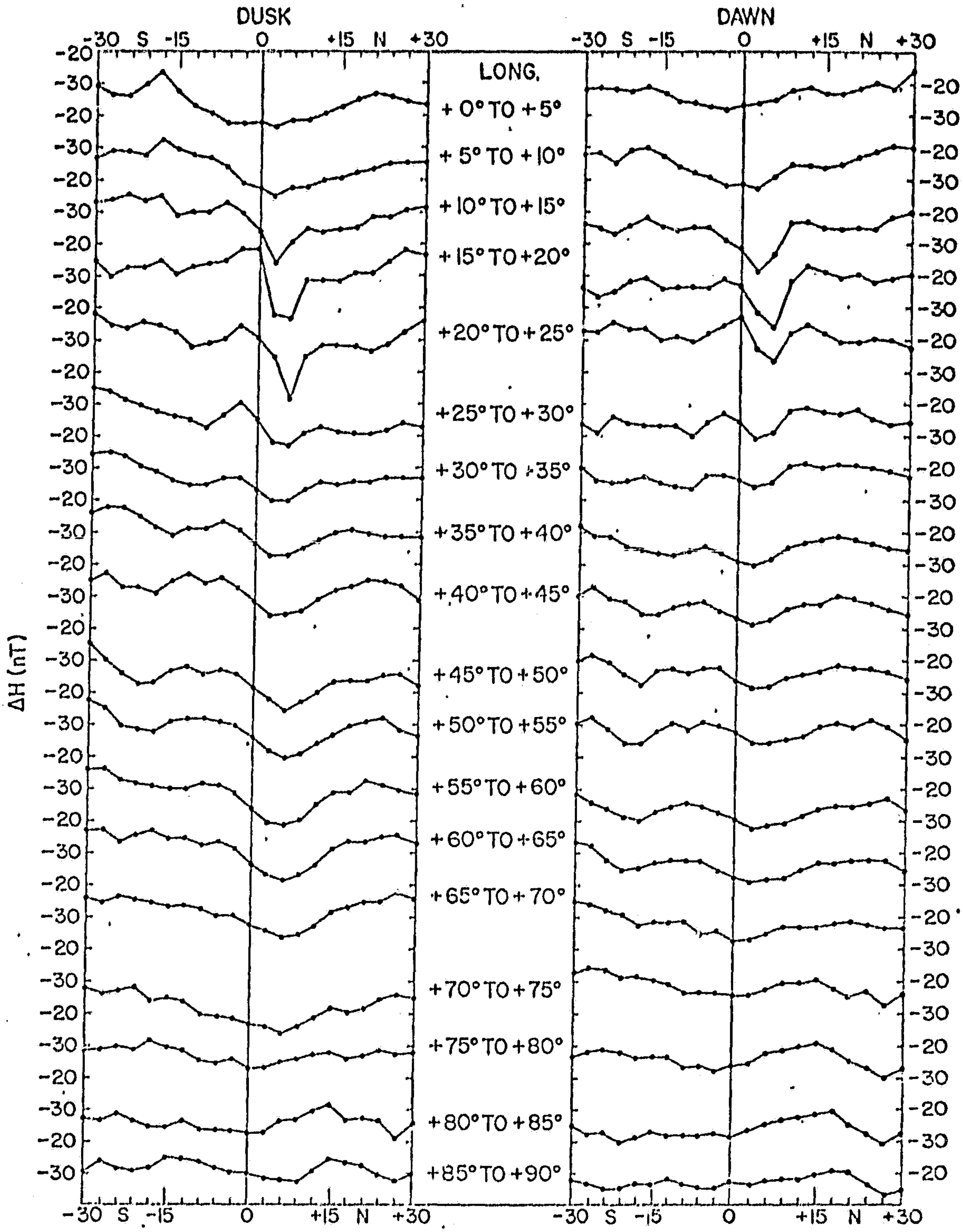
DUSK
DAWN
-30 S -15 0 +15 N +30
LONG.
+0° TO +5°
+5° TO +10°
+10° TO +15°
+15° TO +20°
+20° TO +25°
+25° TO +30°
+30° TO +35°
+35° TO +40°
+40° TO +45°
+45° TO +50°
+50° TO +55°
+55° TO +60°
+60° TO +65°
+65° TO +70°
+70° TO +75°
+75° TO +80°
+80° TO +85°
+85° TO +90°
ΔH (nT)
-20
-30

Fig. 10

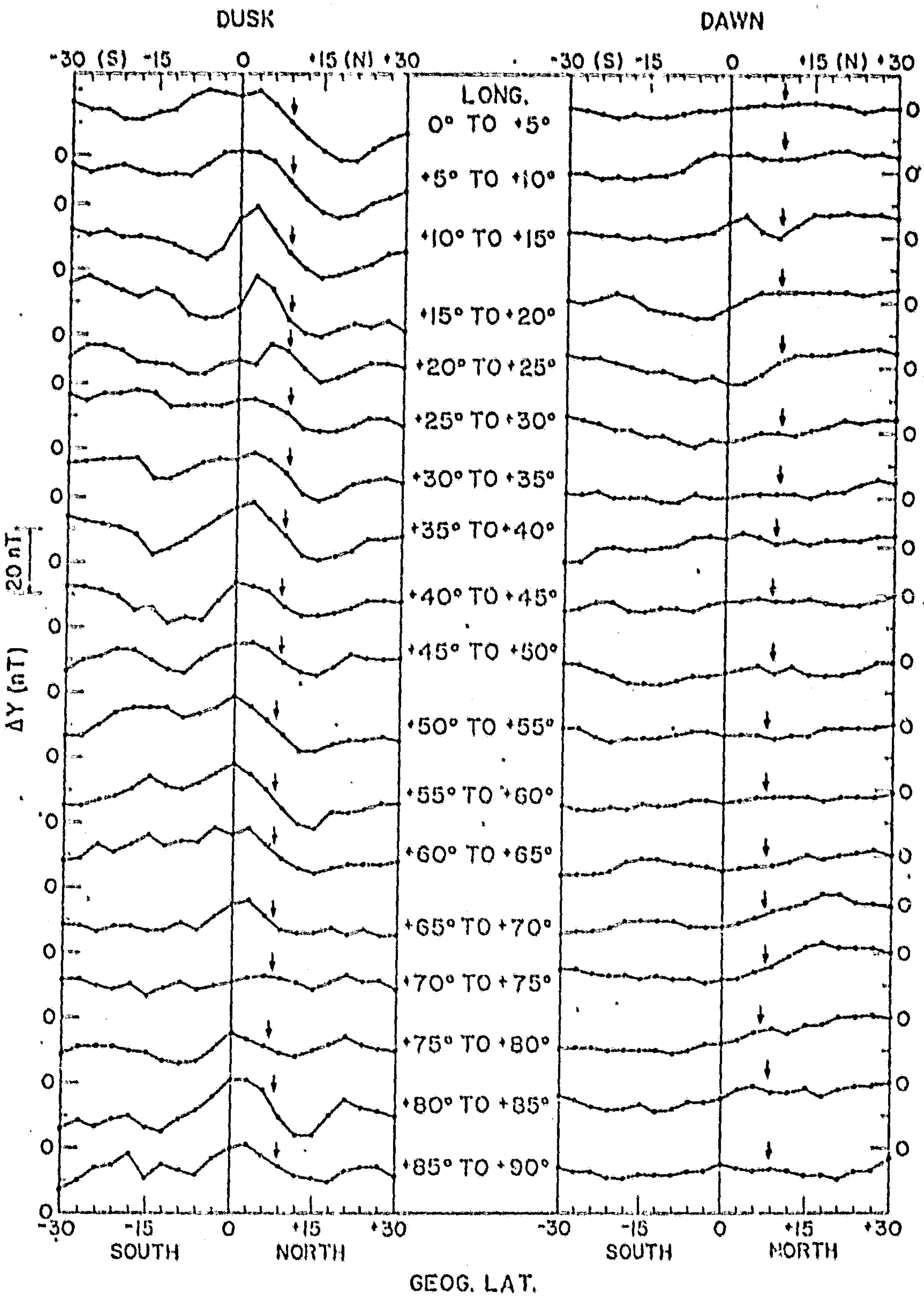
DUSK
DAWN
-30 (S) -15 0 +15 (N) +30
LONG.
0° TO +5°
+5° TO +10°
+10° TO +15°
+15° TO +20°
+20° TO +25°
+25° TO +30°
+30° TO +35°
+35° TO +40°
+40° TO +45°
+45° TO +50°
+50° TO +55°
+55° TO +60°
+60° TO +65°
+65° TO +70°
+70° TO +75°
+75° TO +80°
+80° TO +85°
+85° TO +90°
20 nT
ΔY (nT)
-30 -15 0 +15 +30
SOUTH
NORTH
GEOG. LAT.

Fig. 11

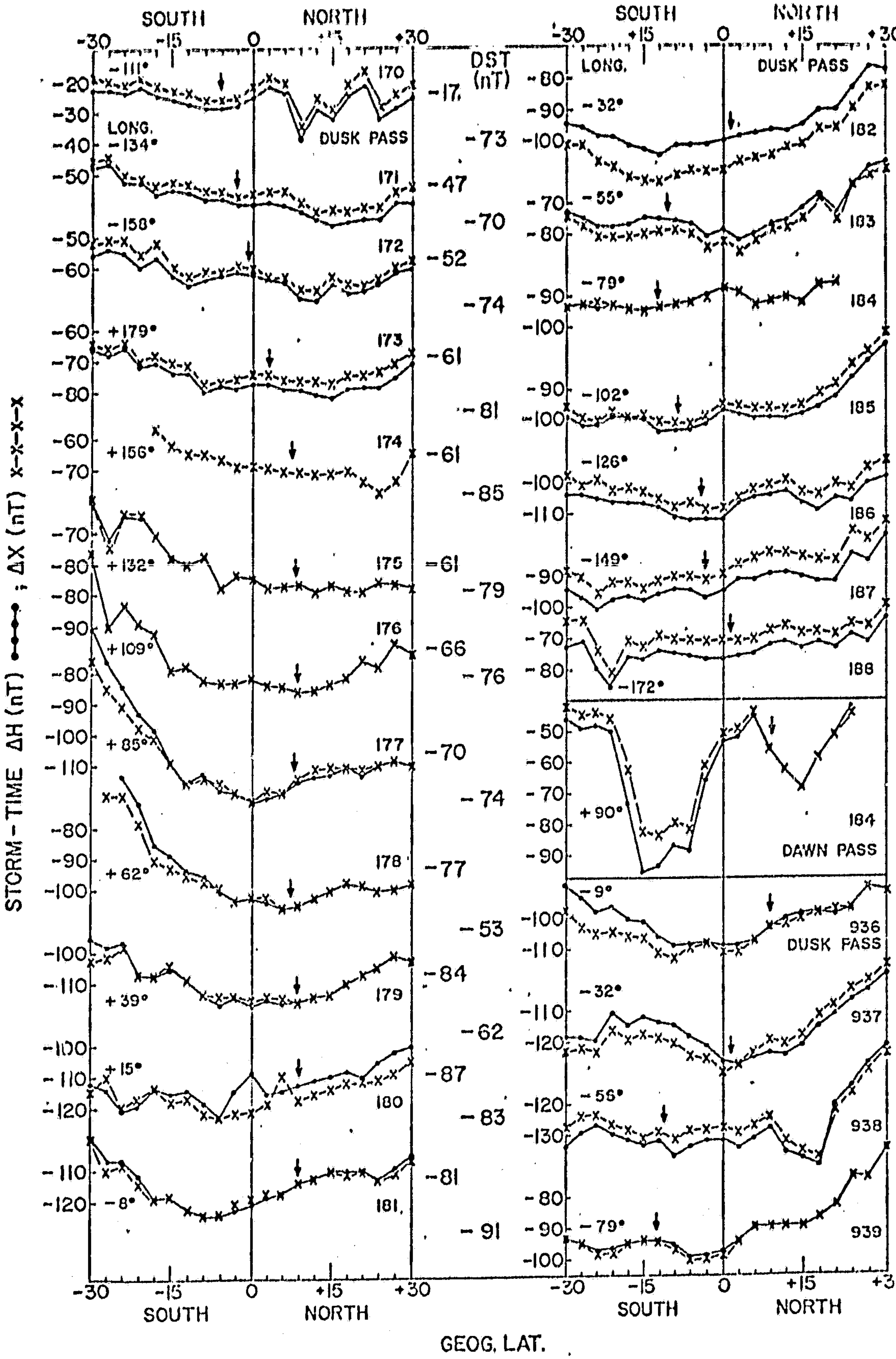
SOUTH
NORTH
DST (nT)
LONG.
DUSK PASS
DAWN PASS
STORM-TIME ΔH (nT) ; ΔX (nT) x-x-x-x
GEOG. LAT.
-111° 170 -17
-134° 171 -47
-158° 172 -52
+179° 173 -61
+156° 174 -61
+132° 175 -61
+109° 176 -66
+85° 177 -70
+62° 178 -77
+39° 179 -84
+15° 180 -87
-8° 181 -81
-73
-70
-74
-81
-85
-79
-76
-74
-53
-62
-83
-91
-32° 182
-55° 183
-79° 184
-102° 185
-126° 186
-149° 187
-172° 188
+90° 184
-9° 936
-32° 937
-56° 938
-79° 939

Fig. 12

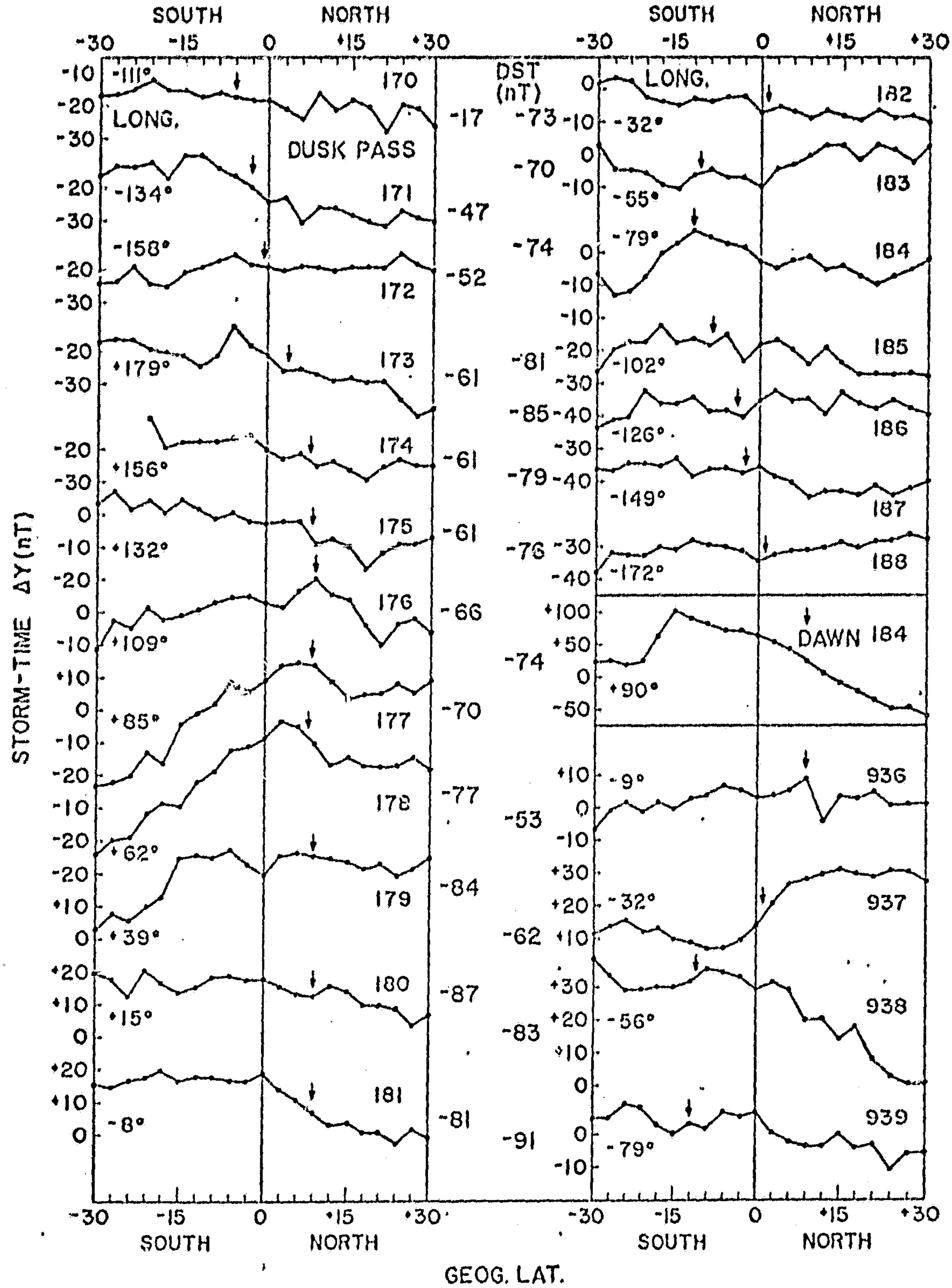
SOUTH
NORTH
DUSK PASS
LONG.
DST (nT)
DAWN 184
STORM-TIME ΔY(nT)
GEOG. LAT.

Fig. 13

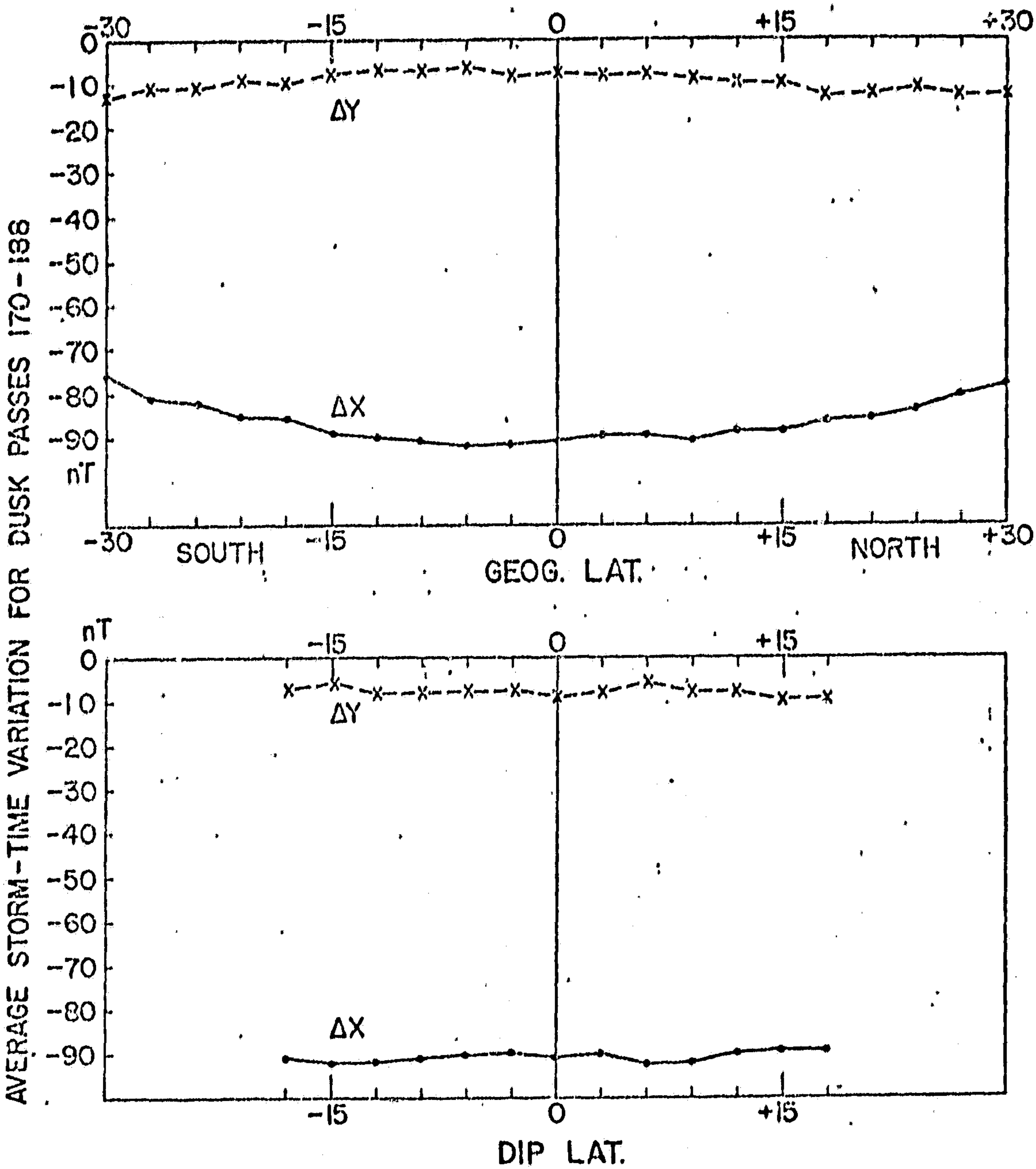
-30
-15
0
+15
+30
0
-10
-20
-30
-40
-50
-60
-70
-80
-90
nT
ΔY
ΔX
-30
SOUTH
-15
0
+15
NORTH
+30
GEOG. LAT.
AVERAGE STORM-TIME VARIATION FOR DUSK PASSES 170-186
nT
-15
0
+15
ΔY
ΔX
-15
0
+15
DIP LAT.

Fig. 14

	Geographic		DAWN PASSES (0600)				DUSK PASSES (1800)			
			Y = Satellite X = Ground		Y = Ground X = Satellite		Y = Satellite X = Ground		Y = Ground X = Satellite	
Station	Lat.	Long.	Corr. Coeff.	Slope(m)	Corr. Coeff.	Slope(m)	Corr. Coeff.	Slope(m)	Corr. Coeff.	Slope(m)
TSUMEB	19.2°S	17.7°E	+ 0.93	1.05 ± 0.08	+ 0.93	0.82 ± 0.07	+ 0.99	0.97 ± 0.03	+ 0.99	1.00 ± 0.03
BANGUI	4.6°N	18.6°E	+ 0.93	1.07 ± 0.08	+ 0.93	0.81 ± 0.05	+ 0.97	0.91 ± 0.04	+ 0.97	1.04 ± 0.05
HERMANUS	34.4°S	19.2°E	+ 0.78	0.85 ± 0.14	+ 0.78	0.71 ± 0.11	+ 0.97	1.10 ± 0.05	+ 0.97	0.85 ± 0.04
SHANGARA	31.8°S	116.0°E	+ 0.85	0.84 ± 0.10	+ 0.85	0.87 ± 0.11	+ 0.81	0.97 ± 0.14	+ 0.81	0.67 ± 0.10
MUNTINLUPA	14.4°N	121.0°E	+ 0.95	1.07 ± 0.07	+ 0.95	0.84 ± 0.06	+ 0.92	0.94 ± 0.03	+ 0.92	0.91 ± 0.07
LUNPING	25.2°N	121.2°E	+ 0.97	0.99 ± 0.05	+ 0.97	0.95 ± 0.05	+ 0.97	0.90 ± 0.05	+ 0.97	1.05 ± 0.05
GUAM	13.4°N	144.9°E	+ 0.97	0.95 ± 0.05	+ 0.97	0.99 ± 0.05	+ 0.98	1.01 ± 0.04	+ 0.98	0.95 ± 0.04
PORT MORESBY	9.4°S	147.1°E	+ 0.96	1.00 ± 0.05	+ 0.96	0.92 ± 0.05	+ 0.97	0.92 ± 0.05	+ 0.97	1.02 ± 0.05
HONOLULU	21.3°N	158.1°W	+ 0.90	0.98 ± 0.09	+ 0.90	0.82 ± 0.08	+ 0.94	1.03 ± 0.06	+ 0.94	0.86 ± 0.06
TAHITI	17.7°S	149.3°W	+ 0.95	0.86 ± 0.05	+ 0.95	1.05 ± 0.07	+ 0.95	0.99 ± 0.05	+ 0.96	0.93 ± 0.05
TUCSON	32.0°N	111.5°W	+ 0.94	0.90 ± 0.06	+ 0.94	0.98 ± 0.07	+ 0.95	0.99 ± 0.07	+ 0.95	0.91 ± 0.06
HUANCAYO	12.1°S	75.3°W	+ 0.92	1.02 ± 0.08	+ 0.92	0.83 ± 0.07	+ 0.92	0.94 ± 0.08	+ 0.92	0.90 ± 0.08
FUQUENE	5.5°N	73.8°W	+ 0.94	1.03 ± 0.08	+ 0.94	0.85 ± 0.06	+ 0.92	0.99 ± 0.08	+ 0.92	0.87 ± 0.07
SAN JUAN	18.1°N	66.2°W	+ 0.96	0.84 ± 0.05	+ 0.96	1.10 ± 0.06	+ 0.95	0.93 ± 0.06	+ 0.95	0.97 ± 0.07
VASSOURAS	22.4°S	43.6°W	+ 0.88	0.73 ± 0.08	+ 0.88	1.05 ± 0.11	+ 0.95	0.89 ± 0.05	+ 0.95	1.03 ± 0.06
M'BOUR	14.4°N	17.0°W	+ 0.97	0.95 ± 0.05	+ 0.97	0.99 ± 0.05	+ 0.98	0.99 ± 0.04	+ 0.98	0.97 ± 0.04
Average				0.946 ± 0.015		0.912 ± 0.015		0.957 ± 0.015		0.935 ± 0.015

Table 1